PAPER-BASED DEVICE FOR WATER ANALYSIS

ALICHA MARUT

A THESIS SUBMITTED IN PARTIAL FULFILLMENT OF
THE REQUIREMENTS FOR MASTER DEGREE OF SCIENCE
IN CHEMISTRY
FACULTY OF SCIENCE
BURAPHA UNIVERSITY
2024

อุปกรณ์แบบกระดาษเพื่อการวิเคราะห์น้ำ

อลิชา เมรุด

วิทยานิพนธ์นี้เป็นส่วนหนึ่งของการศึกษาตามหลักสูตรวิทยาศาสตรมหาบัณฑิต
สาขาวิชาเคมี
คณะวิทยาศาสตร์ มหาวิทยาลัยบูรพา
2567

PAPER-BASED DEVICE FOR WATER ANALYSIS

ALICHA MARUT

A THESIS SUBMITTED IN PARTIAL FULFILLMENT OF
THE REQUIREMENTS FOR MASTER DEGREE OF SCIENCE
IN CHEMISTRY
FACULTY OF SCIENCE
BURAPHA UNIVERSITY
2024

The Thesis of Alicha Marut has been approved by the examining committee to be partial fulfillment of the requirements for the Master Degree of Science in Chemistry of Burapha University

Advisory Committee

Principal advisor

Y. Sameenoi

(Associate Professor Dr. Yupaporn Sameenoi)

Examining Committee

..... Principal examiner

(Associate Professor Dr. Purim Jarujamrus)

Napa T. ..... Member

(Assistant Professor Dr. Napa Tangtreamjitmun)

Y. Sameenoi ..... Member

(Associate Professor Dr. Yupaporn Sameenoi)

P. Usavadee ..... Dean of the Faculty of Science

(Associate Professor Dr. Usavadee Tuntiwaranuruk)

April 23, 2024

This Thesis has been approved by Graduate School Burapha University to be partial fulfillment of the requirements for the Master Degree of Science in Chemistry of Burapha University

Witawat Jangiam ..... Dean of Graduate School

(Associate Professor Dr. Witawat Jangiam)

4 December, 2024

65910108: MAJOR: CHEMISTRY; M.Sc. (CHEMISTRY)

KEYWORDS: PAPER-BASED DEVICES; WATER QUALITY; WATER HARDNESS; CHLORIDE; HEAVY METALS; SIMULTANEOUS ANALYSIS

ALICHA MARUT : PAPER-BASED DEVICE FOR WATER ANALYSIS. ADVISORY COMMITTEE: YUPAPORN SAMEENOI, Ph.D. 2024.

A novel paper-based analytical device has been developed to simultaneously determine water hardness, chloride, and iron in real water samples with radial distance-based measurement. Water hardness was detected using Eriochrome Black T (EBT) assay. Chloride was detected based on the reverse-Mohr precipitation titration. Iron was detected using bathophenanthroline (Bphen). The circular device is divided into three zones, facilitating readings based on radial distances for the three assays at the same time. Specific reagents coating on the detection zone for individual analyte detection was carried out using optimal condition. Water samples were analyzed by adding 75 μL of standard/sample solution to the inlet. As the water sample flows into the sample inlet and diffuses radially outward, the analyte reacts with the reagents, producing a colored band whose radial distance is proportional to the analyte concentration in the water sample. After 3 minutes, the radial distance can be simply measured using either a ruler or ImageJ program to quantify water hardness, chloride, and iron in water. The developed method gave limit of detection for total hardness, chloride and iron of 13 mg/L $CaCO_3$, 0.25 mM and 0.5 mg/L, respectively. The linear range obtained from total hardness, chloride and iron detections were 25-1501 mg/L $CaCO_3$, 1-100 mM and 0.5-300 mg/L, respectively. The sensor demonstrates high selectivity for simultaneous detection of water hardness, chloride, and iron in various water samples with good agreement with traditional standard methods indicating high accuracy and could be potentially used as on-site water quality assessment in the future.

ACKNOWLEDGEMENTS

First of all, I extend my heartfelt gratitude and sincere appreciation to my advisor, Assoc. Prof. Dr. Yupaporn Sameenoi for her invaluable guidance, unwavering support, encouragement, and insightful advice throughout my study and research journey. Great appreciation is offered to all committee members for thesis defense, Assoc. Prof. Dr. Purim Jarujamrus and Asst. Prof. Dr. Napa Tangtreamjitmun for incorporating feedback, suggestions, and insights, as well as addressing any shortcomings, significantly enhances the completeness of this thesis.

I would like to acknowledge (i) Scholarship Support from Burapha University (ii) the Center of Excellence for Innovation in Chemistry (PERCH-CIC), Commission on Higher Education, Ministry of Education, Thailand (iii) Science Innovation Facility, Faculty of Science, Burapha University for the supports throughout my research. I also would like to thank the Department of Chemistry, Faculty of Science, Burapha University, Thailand where I obtained very good experiences.

I express our gratitude to the teachers of the Chemistry Department, Faculty of Science who helps teach and teach the content of the chemistry subject and conduct chemical operations with intensity and care in order to grow me into a good and qualified scientist.

Finally, I would like to express my gratitude to my father, mother, family and Miss. Benjarat Tasaengtong for their unwavering support and encouragement in every aspect of my life. I am also thankful to my older brothers and friends for their assistance, valuable advice, and constant comfort. The value and benefits of this thesis I would like to express my gratitude to my parents, ancestors, and all benefactors both past and present. Their support has played a crucial role in shaping me into the educated and successful person I am today.

Alicha Marut

TABLE OF CONTENTS

Page

ABSTRACT ..... D

ACKNOWLEDGEMENTS ..... E

TABLE OF CONTENTS ..... F

LIST OF TABLES ..... K

LIST OF FIGURES L

CHAPTER 1 1

INTRODUCTION 1

1.1 Statements and significance of the problems 1

1.2 Objective 3

1.3 Contribution to knowledge 3

1.4 Scope of study 4

CHAPTER 2 5

LITERATURE REVIEWS 5

2.1 Hard Water 5

2.1.1 Water hardness analysis 5

2.1.1.1 Complexometric Titration 5

2.1.1.2 Determination of Hardness by Colorimetric Method 6

2.2.2 Buffer type 6

2.2.2.1 N-Cyclohexyl-3-aminopropanesulfonic acid (CAPS) buffer 6

2.2.2.2 Glycine buffer 7

2.2 Chloride 8

2.2.1 Chloride Analysis of Water 8

2.2.1.1 Precipitation Titration 8

2.3 Iron 9

2.3.1 Spectrophotometric Determination of Iron 9

2.4 Water quality standards. 10
2.4.1 Water Quality Standards The World Health Organization (WHO) 10
2.4.2 Water Quality Standards in Thailand 11
2.5 Microfluidic system 13
2.6 Microfluidic paper-based analytical devices (μPADs) 15
2.7 Related literature reviews 16
CHAPTER 3 25
METHODOLOGY 25
3.1 Materials and chemicals 25
3.1.1 Materials 25
3.1.2 Chemicals 25
3.1.3 Real Samples 28
3.2 Research plans 28
3.3 Experimental 29
3.3.1 Preparation of solution 29
3.3.1.1 Glycine buffer solution 29
3.3.1.2 CAPS buffer solution (1 M, pH 10) 29
3.3.1.3 NH_3/NH_4Cl buffer solution 29
3.3.1.4 Eriochrome Black T (EBT) solution 29
3.3.1.5 Magnesium chloride ($MgCl_2$) solution 29
3.3.1.6 Calcium chloride ($CaCl_2$) solution 29
3.3.1.7 Sodium Hydroxide (NaOH) solution 29
3.3.1.8 Hydrochloric Acid (HCl) solution 30
3.3.1.9 Sodium chloride (NaCl) solution 30
3.3.1.10 Potassium Chloride (KCl) solution 30
3.3.1.11 Lithium chloride (LiCl) solution 30
3.3.1.12 Mercury (II) chloride ($HgCl_2$) solution 30
3.3.1.13 Aluminum chloride hexahydrate solution 30

3.3.1.14 Zinc chloride ($ZnCl_2$) solution 30
3.3.1.15 Copper (Cu) solution 30
3.3.1.16 Nickel (Ni) solution 30
3.3.1.17 EDTA solution 30
3.3.1.18 Eriochrome Black T (EBT) indicator solution 31
3.3.1.19 Silver nitrate ($AgNO_3$) solution 31
3.3.1.20 Chromate ($Cr_2O_4^{2-}$) solution 31
3.3.1.21 Sodium chloride (NaCl) solution.....31
3.3.1.22 Sodium Hydrogen Carbonate ($NaHCO_3$) solution 32
3.3.1.23 Potassium Chromate (K_2CrO_4) indicator solution.....32
3.3.1.24 Iron (Fe^{2+}) solution 32
3.3.1.25 Iron (Fe^{3+}) solution 32
3.3.1.26 Fluoride (F^-) solution 32
3.3.1.27 Phosphate (PO_4^{3-}) solution 32
3.3.1.28 Sulfate (SO_4^{2-}) solution 32
3.3.1.29 Bicarbonate (HCO_3^-) solution.....33
3.3.1.30 Polyethylene Glycol (PEG) solution 33
3.3.1.30 Acetate buffer solution (1 M, pH 4.5) 33
3.3.1.31 Hydroxylamine solution 33
3.3.1.32 Bathophenanthroline (Bphen) solution 33
3.3.1.33 Cobalt (Co^{2+}) solution 33
3.3.2 General procedure for device fabrication and simultaneous detection of water hardness, chloride and iron in water.....34
3.3.2.1 General procedure of the paper-based device fabrication 34
3.3.2.2 General procedure for simultaneous analysis of water hardness and chloride in water using the developed paper-based device....34
3.3.3 Design and fabrication of paper-based devices.....35
3.3.3.1 Design of paper-based device for a single analysis.....35
3.3.3.2 Design of paper-based device for a simultaneous analysis 36

3.3.4 Optimization 36
3.3.4.1 Water hardness assay 36
3.3.4.2 Chloride assay 41
3.3.4.3 Iron assay 42
3.3.5 Analytical features 42
3.3.5.1 Linear range 42
3.3.5.2 Repeatability 43
3.3.5.3 Limit of detection (LOD) 43
3.3.6 Interference Studies 43
3.3.7 Storage Stability Study 44
3.3.8 Sample analysis 44
3.3.9 Diameter measurement analysis with ImageJ software 45
3.3.10 Traditional titration method for water hardness and chloride analysis. . 46
CHAPTER 4 47
RESULTS AND DISCUSSION 47
4.1 The principle of the proposed assay 47
4.2 Optimization of the proposed assay 48
4.2.1 Water hardness assay 48
4.2.1.1 Type of buffer 48
4.2.1.2 Reagent deposition sequence and lamination 49
4.2.1.3 Reagent deposition method for simultaneous analysis 50
4.2.1.4 Concentration of buffer 51
4.2.1.5 Glycine buffer range 52
4.2.1.6 EBT concentration 53
4.2.2 Chloride assay 54
4.2.2.1 Reagent deposition method 54
4.2.3 Iron assay 54
4.2.3.1 Concentration of reagent 54

4.3 Analysis of single analyte using the developed paper-based sensors.....55
4.3.1 Water hardness analysis 55
4.3.2 Chloride assay 58
4.3.3 Iron assay.....60
4.4 Interference Studies 64
4.5 Storage Stability Study 66
4.6 Simultaneous analysis of water hardness, chloride and iron 68
CHAPTER 5 73
CONCLUSIONS AND FUTURE PERSPECTIVES 73
5.1 Conclusions.....73
5.2 Future perspective.....74
REFERENCES 75
BIOGRAPHY 80

LIST OF TABLES

Page

Table 1. The water quality parameters standard level for WHO & BIS (HDL - Highest Desirable Limit; MPL- Maximum Permissible Limit) (DWAF, 1996a, 1996b; R. Rajendran1, 2015).....11

Table 2. The water quality parameters standard level in Thailand. 12

Table 3 Tolerance levels for potentially interfering cations. 19

Table 4. Water hardness content obtained from the developed paper-based assay and the traditional titration methods. 57

Table 5. Chloride content in water samples obtained from the developed paper-based devices and Mohr precipitation titration. 59

Table 6. Iron analysis in water samples using the developed paper-based assay and the spectrophotometric assay. 62

Table 7. Analytical figures of merit for water hardness, chloride, and iron detection using developed paper-based devices. 63

Table 8. Radial distance of the water samples tested by the developed paper-based devices. (n=3).....71

Table 9. Water hardness, chloride, and iron contents in water samples obtained from simultaneous analysis using developed paper-based assays and the traditional assay (n = 3). 72

LIST OF FIGURES

Page

Figures 1-1 (A) Radial-distance based paper device for simultaneous analysis of water (B) The measurement procedure for water quality assessment using the developed paper-based device. 3

Figures 2-1 Structure of N-Cyclohexyl-3-aminopropanesulfonic acid (CAPS). 7

Figures 2-2 Structure of Glycine 7

Figures 2-3 Reaction of iron (II) with 1,10-phenanthroline. (Koronkiewicz, 2021) ... 10

Figures 2-4 Schematic representation of µPADs, capillary action of yellow dye in µPADs and rapid color change in the detection zone. (Sriram et al., 2017) 15

Figures 2-5 Schematic of an analytical device using the microfluidic paper-based analytical device (µPAD) for the detection of the total hardness of the water. (a) The principle of the complex titration reaction. (b) The multilayer deposition of the analyte on the device (µPAD). (c) A qualitative examination of the total hardness of the water. (d) A quantitative determination of the total hardness of the water. (Oyewunmi et al., 2020). 16

Figures 2-6 Paper-based analytical devices for water hardness using the titration assay. (Karita & Kaneta, 2016) 17

Figures 2-7 (a) Steps of device fabrication with printing technology for Ca^{2+} testing. (b) Distance-based µPAD design for nano optode-based for Ca^{2+} detection. (c) the dimention of the paper-based device. (Shibata, Hiruta, & Citterio, 2019) 18

Figures 2-8 Images of a paper-based device obtained from the study of the interfering cations on the analysis of Ca^{2+}. (Shibata et al., 2019) 19

Figures 2-9 Distance-based determination of chloride content on µPADs and solubility of silver chromate versus silver chloride. (Rahbar, Paull, & Macka, 2019) 21

Figures 2-10 The effect of shape designs on the standard chloride detection. (Rahbar et al., 2019) 21

Figures 2-11 Correlation curve between apparent distance-based (mm) and chloride concentration (mM) obtained from chloride measurements with various shape of µPADs. (Rahbar et al., 2019) 21

Figures 2-12 Paper-based device for chloride analysis in water. (A) Fabrication of a ready-to-use paper sensor for chloride. (B) Chloride detection procedure using the developed paper sensor. (Tasangtong et al., 2024).....22

Figures 2-13 Device assembly and operation for simultaneous analysis of heavy metals. (Aryal, Brack, Alexander, & Henry, 2023).....23

Figures 2-14 Schematic of distance-based detection in multi-layer devices for heavy metals in water. (Cate, Noblitt, Volckens, & Henry, 2015) 24

Figures 3-1 Research plans. 28

Figures 3-2 The fabrication paper-based device fabrication for simultaneous analysis.34

Figures 3-3 The measurement procedure for water quality assessment using microfluidic paper-based analytical device (μPAD) with radial distance-based measurement. 35

Figures 3-4 The paper-based devices for single analyte analysis designed by the Microsoft word office 365 program. 35

Figures 3-5 The paper-based devices for simultaneous analysis. 36

Figures 3-6 Two-step reagent deposition process on a paper-based device for water hardness analysis (Two layers, without lamination plastic).....37

Figures 3-7 The lamination method for a paper-based device deposited by two-step reagents. 38

Figures 3-8 Schematic diagram showing the fabrication of a paper-based device for water hardness analysis (One-step, without lamination plastic). 38

Figures 3-9 Schematic diagram showing the fabrication of a paper-based device for water hardness analysis (One-step, lamination plastic). 39

Figures 3-10 Schematic diagram showing fabrication a paper-based device for water hardness analysis by dropping the solution into the paper-based device (One-step, lamination plastic).....40

Figures 3-11 Schematic diagram showing fabrication a paper-based device for water hardness analysis by dipping the solution into the paper-based device (One-step, lamination plastic). 40

Figures 4-1 The complex reaction between EBT and Ca^{2+}, Mg^{2+}. 47

Figures 4-2 The precipitation reaction of silver chromate with chloride.....47

Figures 4-3 Reaction between Fe^{2+} and Bathophenanthroline reaction.....48

Figures 4-4 Selecting the type of buffer for water hardness analysis. (A) NH_3/NH_4Cl buffer solution (1.1 mM, pH 10) (B) CAPS buffer solution (1M, pH 10), (C) Glycine buffer solution (0.4 M, pH 10).....49

Figures 4-5 (A) Two-step glycine buffer solution (0.40 M, pH 10) before test with 0.8 mM of Ca^{2+} and Mg^{2+} (B) Two-step glycine buffer solution after test. (C) One-step glycine buffer solution (0.40 M, pH 10) before test with 0.8 mM of Ca^{2+} and Mg^{2+} (D) One-step glycine buffer solution after test. (E) One-step for without lamination plastic. (F) One-step for lamination plastic.....50

Figures 4-6 Study the effect of reagent deposition on a paper-based device. (A) Dropping 100 µL of 0.5 mM EBT + glycine buffer solution (pH 10, 0.48 mM). (B) Dipping device to 0.5 mM EBT + glycine buffer solution (pH 10, 0.48 mM). (C) Tapping device for simultaneous analysis. 51

Figures 4-7 Study the concentration of 0.5 mM EBT + Glycine buffer solution pH 10 (A) concentration 0.40 M (B) concentration 0.48 M (tested with mixed solution of 0.5 mM Ca^{2+}+Mg^{2+}).....52

Figures 4-8 Study the effect of the pH of the glycine buffer solution. 52

Figures 4-9 The study of optimal concentration of Eriochrome black in the concentrations of 0.1, 0.5, 1, and 2 mM. 53

Figures 4-10 Study the effect of reagent deposition on a paper-based device. (A) Dropping $AgNO_3$ solution let dry and then dip the device into $Cr_2O_4^{2-}$ solution (pH 7.2, 50 mM). (B) Dipping the device in 100 µL of $AgNO_3$ solution and letting it dry, then dipping into $Cr2O_4^{2-}$ solution (pH 7.2, 50 mM). (C) Tapping device for simultaneous analysis.....54

Figures 4-11 Study the optimal concentration of Bphen on the paper-based device for Fe^{2+} analysis.....55

Figures 4-12 Measuring radial distance signal on the developed paper-based devices at (A) The central area (B) Edge area. 55

Figures 4-13 A plot of radial distance of the magenta color as a function of $CaCO_3$ in the range of 13-1001 mg/L. (n = 6). (Inset) Linear range of calibration from 25-1501 mg/L (R^2 = 0.9919 for central area measurement and R^2 = 0.9854 for edge area measurement).....57

Figures 4-14 Plot of radial distance as a function of chloride concentration (n = 6). (Inset: a linear range of calibration from 1-100 mM (R^2 = 0.9984 of central area and R^2 = 0.9907 of edge area) 59

Figures 4-15 Plot of radial distance as a function of Fe^{2+} concentration (n = 3) with a linear range of 0.5-300 mg/L (R^2 = 0.9939 of central area and R^2 = 0.9758 of edge area)..... 61

Figures 4-16 Interference study for all three assays. (A) 1:1 and 1:10 mM ratios. (B) 1:0.05, 1:0.1 and 1:10 mM ratios. (C) 1:1 and 1:10 mg/L ratios. Red bars indicate signal changes..... 65

Figures 4-17 Storage stability of paper-based devices in all three tests (n=3) when kept in Fridge at 6-10°C and Room Temperature in the Dark (RT Dark) at 25-38°C..... 67

Figures 4-18 (A) 12.5 mM $AgNO_3$, Chromate Buffer (pH 7.2, 50 mM) with 1 mM Cl^- using deionized water. (B) 12.5 mM $AgNO_3$, Chromate Buffer (pH 7.2, 50 mM) with 1 mM Cl^- using acid deionized water. (C) 12.5 mM $AgNO_3$, Chromate Buffer (pH 7.2, 100 mM) with 7 mM Cl^- using deionized water. (D) 12.5 mM $AgNO_3$, Chromate Buffer (pH 7.2, 100 mM) with 1 mM Cl^- using acid deionized water 68

Figures 4-19 Simultaneous analysis of water hardness, chloride, and iron in real water samples. (A) Paper-based device developed before testing with the samples. (B) The device after testing with water samples without pH adjustment. (C) The device after testing with water samples with the pH adjusted to 4.5. (D) The device after testing with water samples with the pH adjusted to 4.5 and spiked with 1 mg/L Fe^{2+}standard solution..... 70

CHAPTER 1
INTRODUCTION

1.1 Statements and significance of the problems

Water is a precious resource for humanity and is utilized for various purposes such as drinking, domestic use, industrial use, and agriculture, which is the ultimate source of food for all. Assessing water quality often hinges on the levels of hardness, chloride, and iron present. (Jayaraman, Nagarajan, Partheeban, & Krishnamurthy, 2024; Oyewunmi, Safiabadi-Tali, & Jahanshahi-Anbuhi, 2020) These ions are abundant in natural water, thus their detection holds significant importance.(J. Bartram, 1999) Overconsumption or exposure to these ions can harm the environment and human health, leading to issues like scaling, corrosion, and rust in pipes, faucets, and appliances like dishwashers, washing machines, and coffee makers. This can impair performance and cause premature equipment failure. Additionally, it may contribute to various health conditions such as Hypercalcemia, Chronic kidney disease, Immune deficiency, Hypertension, Atherosclerosis, liver damage, Slow coagulopathy and more than that, it can be life-threatening.(AL-KHATEEB, 2014; Dvorak, 2021; Gaur et al., 2022; Gwak et al., 2021; Sengupta, 2013)

Therefore, regular water quality testing is essential. The World Health Organization (WHO) has set the maximum permissible concentrations of total hardness, chloride, and iron in water as follows: 300 mg L^{-1}, 250 mg L^{-1}, and 0.3-10 mg L^{-1}, respectively.(R. Rajendran1, 2015) Therefore, monitoring of ion levels is crucial across environmental, industrial, and public health domains.

Traditional methods of water analysis include precipitation titration, ion chromatography,(University of Canterbury; Wu, Hu, Liu, & Zhang, 2021) complexometric titrations, (© The Open University, 2019) and spectrophotometry.(Hiroki Tamura, 1974) These techniques are highly selective and sensitive, featuring low detection limits and the ability to detect multiple elements simultaneously. However, they are usually conducted in laboratories by trained personnel, which can be time-consuming and expensive, posing challenges for public access. (Nouanthavong, Nacapricha, Henry, & Sameenoi, 2016; Taprab & Sameenoi,

2019) Therefore, there is a demand for a low-cost, easy-to-fabricate device that can quickly detect ions, is portable, user-friendly, and environmentally sustainable.

Microfluidic paper-based analytical devices (μPADs) are a type of microfluidic platform that uses paper as a substrate for chemical and biological analysis. μPADs have gained popularity due to their low cost, portability, and simplicity in design and operation. They consist of hydrophilic channels and wells created by printing wax or polymer on hydrophobic paper. The channels and wells can be loaded with samples and reagents to perform various assays such as colorimetric, (Sharifi, Tashkhourian, & Hemmateenejad, 2020) fluorescent, (Gemma Aragay, 2012) electrochemical and immunoassays. (Bigham et al., 2019) In the past, several paper-based assays have been created to quickly and easily evaluate water quality. These assays include the colorimetric detection of water hardness and the distance-based detection of chloride. However, they can only detect one analyte at a time. Therefore, there is a need for the simultaneous detection of multiple ions to offer several advantages including increased efficiency, cost-effectiveness, comprehensive analysis, greater accuracy, and real-time monitoring of water quality. (Sriram et al., 2017)

This study aimed to develop a paper-based device that can detect multiple ions simultaneously, to assess water quality. The device consisted of a circular shape and was divided into three zones, as shown in Figure 1A. The measurement procedure for water quality assessment using a microfluidic paper-based analytical device (μPAD) with radial distance-based measurement, as shown in Figure 1B. This design allowed for radial distance-based readout, enabling the detect multiple ions simultaneously. The device's detection zones were coated with specific reagents to detect each analyte for water quality assessment. In this research, water hardness (Ca^{2+}/Mg^{2+}), chloride (Cl^{-}), and iron (Fe^{2+}) were detected simultaneously. Once all the reagents are deposited, the device was laminated and a 0.5-mm hole was cut in the center of the top lamination film to serve as a sample inlet. To detect multiple analyte ions simultaneously, the device was immersed in water samples or adding 75 μL water sample into the sample inlet. As the water sample flowed into the sample inlet and diffused radially outward, the analyte reacted with the reagents, producing a colored band whose radial distance was proportional to the analyte concentration in the water sample. The radial distance can be simply measured using either a ruler or ImageJ program. Therefore, the

developed paper-based device provided a rapid, simultaneous, cost-effective, and user-friendly analysis for water quality assessment.

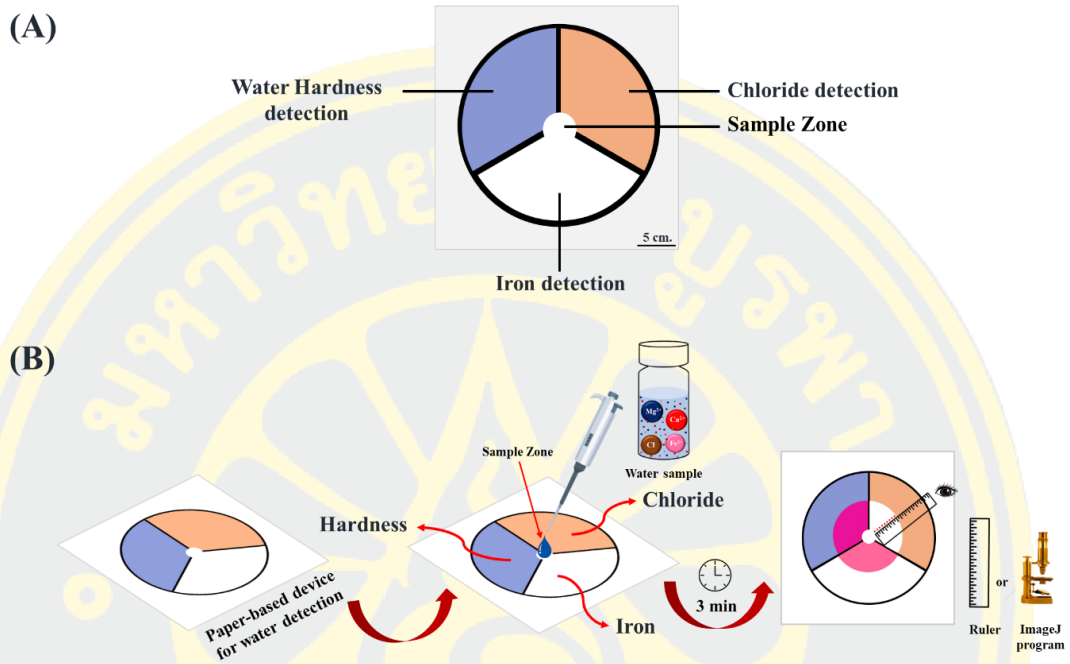

Figures 1-1 (A) Radial-distance based paper device for simultaneous analysis of water (B) The measurement procedure for water quality assessment using the developed paper-based device.

1.2 Objective

To develop a radial distance-based measurement paper device for simultaneous detection of water hardness, chloride and iron in water to assess water quality.

1.3 Contribution to knowledge

The paper-based device developed in this study can simultaneously determine the levels of water hardness chloride and iron in water, utilizing a simple color radial distance-based measurement approach. This enables a quick, cost-effective, user-friendly, and on-site assessment of water quality.

1.4 Scope of study

1. Design and fabricate a paper-based device that can accommodate simultaneous analysis of three parameters and radial distance-based measurement using wax-printing methods.

2. Study the optimization condition to detect water hardness, chloride and iron in water using the developed paper-based devices including reagent concentration, assay pH, interferences and stability of the device.

3. Study the analytical features including linear range, reproducibility, limit of detection (LOD) for the analysis of each parameter using the developed paper-based device with optimal conditions.

4. Apply the developed paper-based devices for simultaneous determination of water hardness, chloride and iron in real water samples and compare the results to those obtained from standard methods to determine the accuracy of the developed assay.

CHAPTER 2
LITERATURE REVIEWS

2.1 Hard Water

Water hardness refers to the level of certain dissolved metallic ions in water, specifically the amount of calcium and magnesium ions present. The hardness of water can be classified as either temporary or permanent. Temporary hardness is caused by the presence of dissolved bicarbonate minerals, which can be removed by boiling the water. Permanent hardness, on the other hand, is caused by the presence of dissolved calcium and magnesium sulfates, chlorides, and nitrates, which cannot be removed by boiling. The concentration of calcium and magnesium ions present in natural water are relatively high compared to other metal ions. Water hardness is therefore basically defined as the total amount of calcium and magnesium ions in the water reported as calcium carbonate equivalents. Accordingly, the World Health Organization (WHO) classifies water hardness into four categories based on calcium carbonate equivalent concentrations (Oyewunmi et al., 2020) as follows:

- Soft water (<0.61 mM)
- Moderately hard water (0.61–1.20 mM)
- Hard water (1.21–1.80 mM)
- Very hard water (>1.80 mM)

2.1.1 Water hardness analysis

2.1.1.1 Complexometric Titration

The theory behind water hardness titration is based on the principle of complexometric titration, which involves the formation of stable complexes between metal ions and a chelating agent, also known as a titrant. Ethylenediaminetetraacetic acid (EDTA) is a commonly used chelating agent in water hardness titrations. EDTA forms a stable complex with calcium and magnesium ions, displacing them from their previous complex formations with other ligands, and thus allowing for their titration with a standardized EDTA solution. (Husain, 2017)

The procedure of water hardness titration typically involves the use of a complexometric indicator, which changes color when the metal ions are completely

complexed by the EDTA. One popular indicator for water hardness titrations is Eriochrome Black T (EBT), which changes from blue to pink as the pH of the solution changes from acidic to slightly basic upon the addition of EDTA. The endpoint of the titration is reached when the pink color persists for a short period of time, indicating that all the calcium and magnesium ions have reacted with the EDTA. (© The Open University, 2019) The chemical reactions involved in hard water titration can be represented as (1) and (2).

$$\text{Indicator-Ca (blue)} + Ca^{2+} \text{ or } Mg^{2+} \longrightarrow \text{Indicator-Ca (red)} \quad \text{.....(1)}$$

$$\text{Indicator-Ca (red)} + \text{EDTA} \longrightarrow \text{EDTA-Ca} + \text{Indicator (blue)} \quad \text{.....(2)}$$

2.1.1.2 Determination of Hardness by Colorimetric Method

The Eriochrome Black T indicator method is a rough estimation of water hardness by directly adding Eriochrome Black T indicator solution into the water sample. If the sample is hard, the solution will turn red or magenta. If there is no hardness, the solution will be blue. However, this test method has a high discrepancy as Eriochrome Black T can also react with Ca^{2+} and Mg^{2+} ions, and the pH of the solution can also affect the color change. Additionally, the presence of red or magenta color does not indicate the exact level of water hardness.

2.2.2 Buffer type

2.2.2.1 N-Cyclohexyl-3-aminopropanesulfonic acid (CAPS) buffer

CAPS buffer, also known as 3-(cyclohexylamino)-1-propanesulfonic acid, has a chemical structure with a cyclic hexyl group attached to an amino and sulfonic acid functional group. CAPS is a zwitterionic buffer, meaning it can exist in both acidic and basic environments, and it maintains its pH within a narrow range, making it an effective buffering agent. CAPS has a pKa value of 10.4, which allows it to be used in a slightly basic pH range, making it particularly suitable for applications where a higher pH is required.

One of the primarily uses of CAPS buffer is in electrophoresis, particularly in protein and nucleic acid gel electrophoresis. CAPS buffer is known for its stability and minimal interference with biological molecules, making it ideal for separating and

analyzing proteins and nucleic acids. CAPS buffer has been shown to provide excellent resolution and separation of proteins in polyacrylamide gel electrophoresis (PAGE) and sodium dodecyl sulfate-polyacrylamide gel electrophoresis (SDS-PAGE) due to its unique buffering capacity and lack of UV absorbance, which minimizes background interference in detection methods such as Coomassie staining or Western blotting. (Hames, 2017; Izzo, 2016)

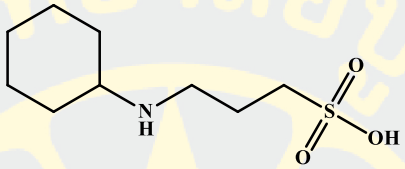

Figures 2-1 Structure of N-Cyclohexyl-3-aminopropanesulfonic acid (CAPS).

2.2.2.2 Glycine buffer

Glycine buffer is a commonly used chemical buffer in various scientific and industrial applications due to its unique properties and versatility. It is a zwitterionic amino acid that can act as both an acidic and a basic buffer, making it suitable for maintaining a stable pH environment in a wide range of biological and chemical processes.

One of the key properties of glycine buffer is its ability to function as an effective pH regulator in a specific range. Glycine has two ionizable groups, a carboxyl group (COOH) and an amino group (NH_2), which can donate or accept protons depending on the pH of the solution. The pKa values of these groups are 2.35 and 9.78, respectively, making glycine buffer effective in the pH range of 2.2 to 3.8 and 9.2 to 10.8, with the optimum buffering capacity around pH 7.4, which is close to the physiological pH of many biological systems. (Akhtar, 2022)

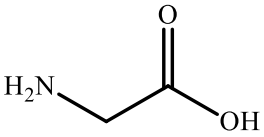

Figures 2-2 Structure of Glycine.

2.2 Chloride

Chloride ion (Cl^-) is a common type of ion found in the environment. Natural water sources, such as rivers, lakes, and groundwater, typically contain chloride, mostly in the form of calcium, magnesium, and sodium chloride. The concentration of chloride in natural water sources varies depending on the location, with seawater having chloride levels as high as 19,000 mg/L, while chloride levels in general surface and groundwater are usually less than 50 mg/L. Chloride plays a crucial role in environmental science and is used in various industrial applications. However, high levels of chloride in water can be detrimental to the environment, human health, and industrial production. Therefore, the measurement of chloride levels in water is of great importance, especially due to the significant amount of pollutants released from household and industrial activities that can result in water pollution. (Wu et al., 2021)

2.2.1 Chloride Analysis of Water

2.2.1.1 Precipitation Titration

Precipitation titration is a titration using $AgNO_3$ solution as the titrant, which can be precipitated with the anions of the halides of interest. This type of titration is sometimes called Argentometric method. The resulting precipitate is low soluble.

This type of titration can be divided into 2 types:

1. Direct titration is a method in which the sample anion solution is directly titrated with a standard solution of $AgNO_3$ from a burette.
2. Indirect titration involves adding an excess amount of $AgNO_3$ standard solution to the analyte solution, and then determining the excess amount of $AgNO_3$ by back titration using a standard solution of sodium thiosulfate ($Na_2S_2O_3$).

The precipitation titration method using silver salt can be divided into three types based on the type of indicator used, as follows:

Mohr's method, also known as silver nitrate titration or chromate titration, is a widely used precipitation titration method that utilizes chromate ions (CrO_4^{2-}) as an indicator to determine the endpoint of the titration. The formation of a red precipitate of silver chromate (Ag_2CrO_4) indicates the endpoint of the titration. Mohr's method is

commonly employed for the determination of chloride ions (Cl^-) in samples, such as saltwater, wastewater, and food samples. A simple and rapid Mohr's titration method was developed for the determination of chloride ions in seawater using silver nitrate as the titrant and chromate ions as the indicator. (Wang, 2021)

Volhard's method, also known as the silver nitrate titration with thiocyanate ions, is another widely used precipitation titration method that utilizes thiocyanate ions (SCN^-) as an indicator to determine the endpoint of the titration. The formation of a reddish-brown precipitate of silver thiocyanate (AgSCN) indicates the endpoint of the titration. Volhard's method is commonly employed for the determination of halide ions, such as chloride, bromide, and iodide ions, in various samples, including water, soil, and pharmaceuticals. (Kaur, 2020)

Fajan's method, also known as the adsorption indicator method, is a unique precipitation titration method that utilizes adsorption indicators, such as fluorides or chlorides, to determine the endpoint of the titration. The adsorption of the indicator ions onto the precipitate surface results in a change in color, which indicates the endpoint of the titration. (Vinutha, 2018)

2.3 Iron

Iron in water refers to the presence of the chemical element iron (Fe) dissolved or suspended in water. This can occur naturally through the weathering of rocks and soil, or it may result from human activities such as industrial processes or corroding pipes. Iron in water can manifest in different forms, including ferrous iron (Fe^{2+}) and ferric iron (Fe^{3+}). While small amounts of iron are typically not harmful and may even be beneficial for health, excessive levels can lead to issues such as discoloration, unpleasant taste, and staining of fixtures and clothing. Therefore, monitoring and controlling iron levels in water are essential to ensure its safety and quality for various uses. (El-Turki, 2017; Korte, Tomsič, Bratkič, Franko, & Budasheva, 2019)

2.3.1 Spectrophotometric Determination of Iron

Iron content is determined using spectrophotometry, where an orange-red complex forms between the Fe^{2+}ion and 1,10-phenanthroline or o-phenanthroline. Complex formation occurs regardless of the solution pH, but it's typically conducted at

around pH 3.5 to avoid iron salt precipitation. Absorbance is then measured at a wavelength of 510 nm. When adding an excess of a reducing agent such as hydroxylamine hydrochloride ($NH_2OH \cdot HCl$), any Fe^{3+} resulting from the reaction between Fe^{2+} and oxygen gas is converted back to Fe^{2+} upon addition of standard Fe^{2+} at different concentrations. The light absorption value is then measured to create a calibration curve, establishing the relationship between complex concentration and absorbance value. This curve is utilized to determine the concentration of Fe^{2+} in the sample solution. The relevant reactions are shown in the equation.

$$4Fe^{3+}(aq) + 2NH_2OH(aq) \rightleftharpoons 4Fe^{2+}(aq) + N_2O(aq) + 4H^{+}(aq) + H_2O(l) \quad \text{.....(1)}$$

$$Fe^{2+}(aq) + 3PhenH^{+}(aq) \rightleftharpoons Fe(Phen)_3^{2+}(aq) + 3H^{+}(aq) \quad \text{.....(2)}$$

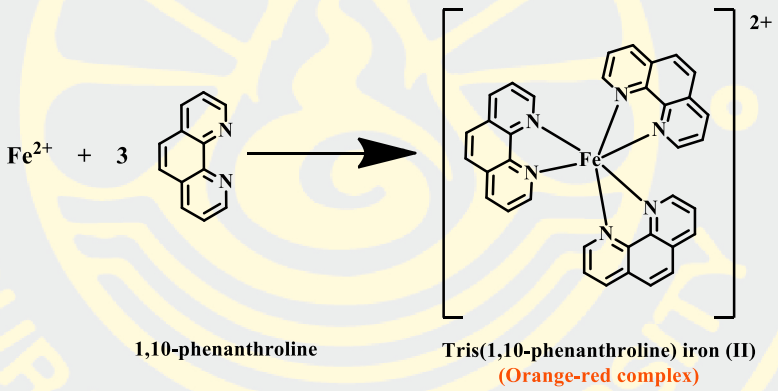

Figures 2-3 Reaction of iron (II) with 1,10-phenanthroline. (Koronkiewicz, 2021)

2.4 Water quality standards.

2.4.1 Water Quality Standards The World Health Organization (WHO)

The World Health Organization (WHO) establishes water quality standards to ensure water safety worldwide. These standards are essential for protecting public health and preventing waterborne diseases. The WHO regularly reviews scientific evidence and updates its guidelines accordingly. Some key parameters and contaminants monitored by WHO for drinking water quality as in table 1.

Table 1. The water quality parameters standard level for WHO & BIS (HDL - Highest Desirable Limit; MPL- Maximum Permissible Limit) (DWAF, 1996a, 1996b; R. Rajendran1, 2015)

Parameters	Units	WHO – standard	
		HDL	MPL
Odour			
Turbidity	NTU	5	10
Total dissolved solids	mg/L	500	2000
Electrical conductivity	µS/cm	Nil	Nil
Chemical parameters			
pH		6.5-9.5	No relaxation
Alkalinity total ($CaCO_3$)	mg/L	200	600
Total hardness ($CaCO_3$)	mg/L	300	600
Calcium (Ca^{2+})	mg/L	75	200
Magnesium (Mg^{2+})	mg/L	30	150
Sodium (Na^{+})	mg/L	Nil	Nil
Potassium (K^{+})	mg/L	Nil	Nil
Iron (Fe^{2+})	mg/L	0.3	1.0
Manganese (Mn^{2+})	mg/L	0.1	0.1
Chromimum (Cr^{3+})	mg/L	Nil	Nil
Nitrite (NO_2)	mg/L	Nil	Nil
Nitrate (NO_3^{-})	mg/L	50	No relaxation
Chloride (Cl^{-})	mg/L	250	1000
Fluoride (F^{-})	mg/L	1	1.5
Sulphate (SO_4^{2-})	mg/L	200	400

2.4.2 Water Quality Standards in Thailand

Water quality standards in Thailand are guidelines set by regulatory bodies to ensure the safety and cleanliness of water resources. These standards establish permissible levels of various pollutants and parameters in water bodies to safeguard human health and the environment. In Thailand, water quality standards are primarily

regulated by the Pollution Control Department (PCD) under the Ministry of Natural Resources and Environment. The standards cover a range of parameters including chemical, physical, and biological aspects of water quality. For instance, the Thai government has established standards for key pollutants such as biochemical oxygen demand (BOD), dissolved oxygen (DO), pH, turbidity, and heavy metals like lead and mercury. These standards are based on scientific research and international best practices, tailored to the specific environmental conditions of Thailand and table 2. show the water quality parameters standard level in Thailand. (Pholprasert, 2002)

Table 2. The water quality parameters standard level in Thailand.

Parameters	**Units**	**Standard Value**
1. Physical characteristics		
Appearance colour	Pt-Co Unit	Not more than 15
Taste and odour	-	-
Turbidity	NTU	Not more than 4
pH	-	6.5-8.5
2. Chemical characteristics		
Total dissolved solids	mg/L	Not more than 600
Iron	mg/L	Not more than 0.3
Manganese	mg/L	Not more than 0.3
Copper	mg/L	Not more than 2.0
Zinc	mg/L	Not more than 3.0
Total hardness ($CaCO_3$)	mg/L	Not more than 300
Sulfate	mg/L	Not more than 250
Chloride	mg/L	Not more than 250
Fluoride	mg/L	Not more than 0.7
Nitrate (NO_3)	mg/L	Not more than 50
Nitrite (NO_2)	mg/L	Not more than 3

Parameters	Units	Standard Value
3. Toxins		
Mercury	mg/L	Not more than 0.001
Lead	mg/L	Not more than 0.01
Arsenic	mg/L	Not more than 0.01
Selenium	mg/L	Not more than 0.01
Chromium	mg/L	Not more than 0.05
Cadmium	mg/L	Not more than 0.003
Barium	mg/L	Not more than 0.7
Cyanide	mg/L	Not more than 0.07

These parameters are regularly monitored through sampling and testing conducted by government agencies and other stakeholders. Non-compliance with water quality standards may result in regulatory actions, including fines, enforcement measures, and public notifications. It's important to note that Thailand's water quality standards may also be influenced by international guidelines, such as those established by the World Health Organization (WHO) and regional bodies like the Association of Southeast Asian Nations (ASEAN).

2.5 Microfluidic system

The microfluidic system involves the design and application of technical systems that manipulate fluids at the microscopic level and the use of small amounts of analytical reagents and reagents. Microfluidics is a new field in diagnostics that allows very precise control and management of fluids. The primary purpose of microfluidics is to integrate with the lab on a chip. Nowadays, most scientific and medical devices are miniaturized to increase the efficiency of an installation with other equipment, convenient to carry, accurate and fast analysis. Microfluidics is a microscopic flow channel (microchannel) which is a small flow channel for different types of liquids or solutions at the microliter level (Liu et al., 2010). For the fabrication method, traditional microfluidic devices were made from glass, silicon, and polymer materials such as poly(dimethyl siloxane) (PDMS) (Nilghaz et al., 2012). However, these materials are expensive and the manufacturing process is complicated.

Over recent years, an alternative material used to create microfluidic devices is based on cellulose fiber such as paper and cloth because cellulose-based material is worldwide available and inexpensive. It can be developed for rapid and on-site analysis, disposal, and biocompatibility and most importantly, use a small number of reagents. These are called microfluidic paper-based analytical devices (µPADs). µPADs are constructed by forming the device's hydrophilic and hydrophobic barrier through various methods. There are several techniques used to create a hydrophobic barrier on paper-based devices, such as Wax printing, Inkjet printing, Wax dipping, Photolithography and Wax screen printing. (Yetisen, Akram, & Lowe, 2013) Paper-based microfluidics as a microfluidic device has several advantages which are the simple to fabricate, low-cost, and fast analysis. µPADs are currently being used in medical diagnostics, food science and the environmental monitoring.

Fabrics have recently been used to develop microfluidic devices. Fabric is a material that is ubiquitous, and easily available. It also has several attractive features, such as small, inexpensive, lightweight, portable good biocompatibility and biodegradability, portability and can be used on-site. (Tasaengtong & Sameenoi, 2020). However, there are not many methods for creating µCAD. Each method has different advantages and limitations. Therefore, the development of fabrication method of this fabric device is currently of interest.

2.6 Microfluidic paper-based analytical devices (µPADs)

Microfluidic paper-based analytical devices (µPADs) are a new class of analytical technology that have been applied in various fields including point-of-care diagnostic, clinical diagnostics, food and environmental safety. The major advantages of this technology is that the cost is affordable, the analysis is rapid, portable, disposable, biocompatible and provide the use in developing countries.

The paper-based device was first introduced in 2007 by Martinez et al. There are two components of the paper-based device including hydrophilic and hydrophobic. The hydrophilic portion is where the reaction occurs and the hydrophobic barrier defines the test zone. The

hydrophobic barrier can be made using a variety of approaches, such as wax printing, inkjet printing, wax dipping, photolithography, and wax screen-printing. (Yetisen et al., 2013)

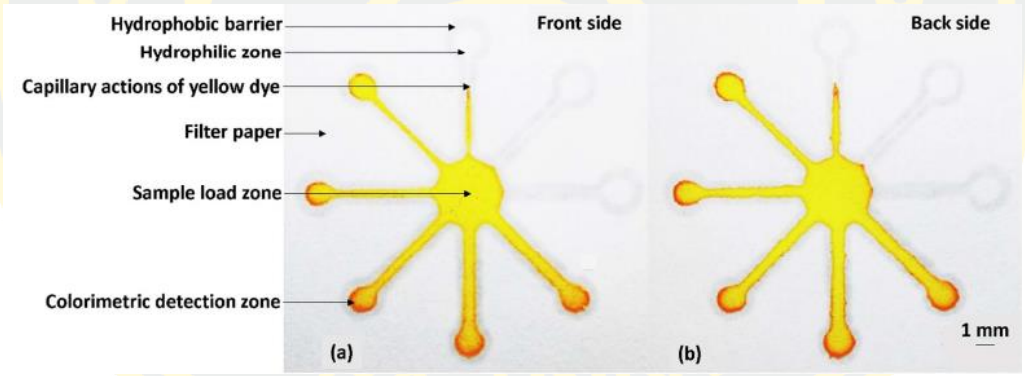

Figures 2-4 Schematic representation of µPADs, capillary action of yellow dye in µPADs and rapid color change in the detection zone. (Sriram et al., 2017)

2.7 Related literature reviews

Oyewunmi, Safiabadi-Tali, & Jahanshahi-Anbuhi, (2020) have reported the development of a dip-and-read paper-based analytical device (µPAD) for the qualitative and quantitative detection of water hardness. The device was fabricated using a combined wax printing method to create a hydrophobic barrier and a hydrophilic region for the reaction. The µPAD has five reaction and sensing zones, which can classify water hardness according to the definitions provided by the World Health Organization (WHO), including soft water, moderately hard water, hard water, and very hard water. The color changes from blue to pink within three minutes, allowing for rapid observation of results. One notable feature of the developed µPAD is that it does not require the use of ethylenediaminetetraacetic acid (EDTA), making it more efficient compared to other methods that rely on this chemical. The calculated limit of detection (LOD) for the developed µPAD is 0.2 mM, which is at least 80% lower than other commonly reported test strips and paper-based analytical devices (µPADs), indicating its high sensitivity for detecting water hardness.

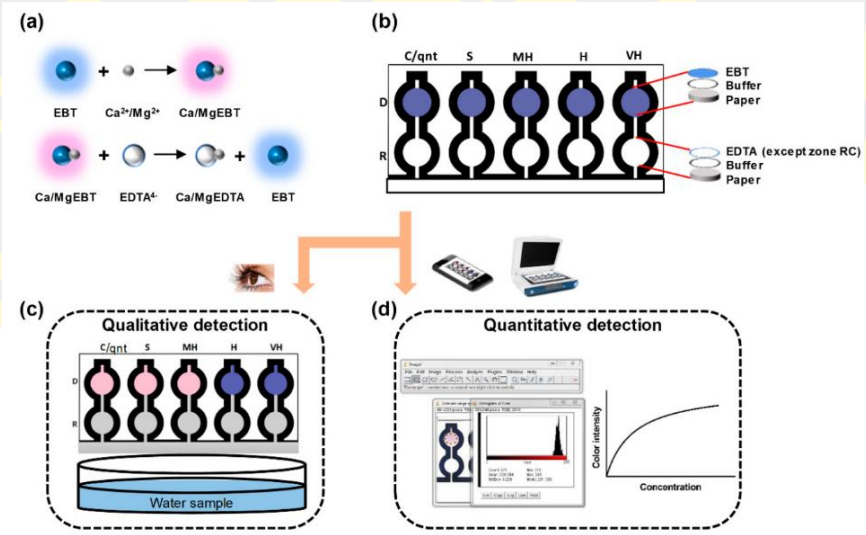

Figures 2-5 Schematic of an analytical device using the microfluidic paper-based analytical device (µPAD) for the detection of the total hardness of the water. (a) The principle of the complex titration reaction. (b) The multilayer deposition of the analyte on the device (µPAD). (c) A qualitative examination of the total hardness of the water. (d) A quantitative determination of the total hardness of the water. (Oyewunmi et al., 2020).

Karita & Kaneta, (2016) have developed paper-based analytical devices for the rapid determination of water hardness using chelate titrations of calcium and magnesium in water. A titration paper-based analytical device was fabricated to contain multiple reaction zones and detection zones connected to the sample zone allows for convenient and efficient testing of water hardness levels. The analysis of water harness is based on chelating titration of calcium and magnesium and Ethylenediaminetetraacetic acid (EDTA) at pH 10 or 13 adjusted by N-Cyclohexyl-3-aminopropanesulfonic acid (CAPS) buffer preloaded into the paper-based device. Different amounts of EDTA are loaded into the reaction zone, and Eriochrome Black T or Calcon is added to the detection zone. The concentration and volume of the reagents in each zone are carefully designed to enable the quantification of calcium and magnesium ions. The developed method provides detection with a relatively high detection limit of 0.5 mM, which may not be sensitive enough for certain applications. However, the low-cost nature of the paper-based device makes it suitable for use in developing countries or resource-limited settings where access to sophisticated analytical equipment may be limited.

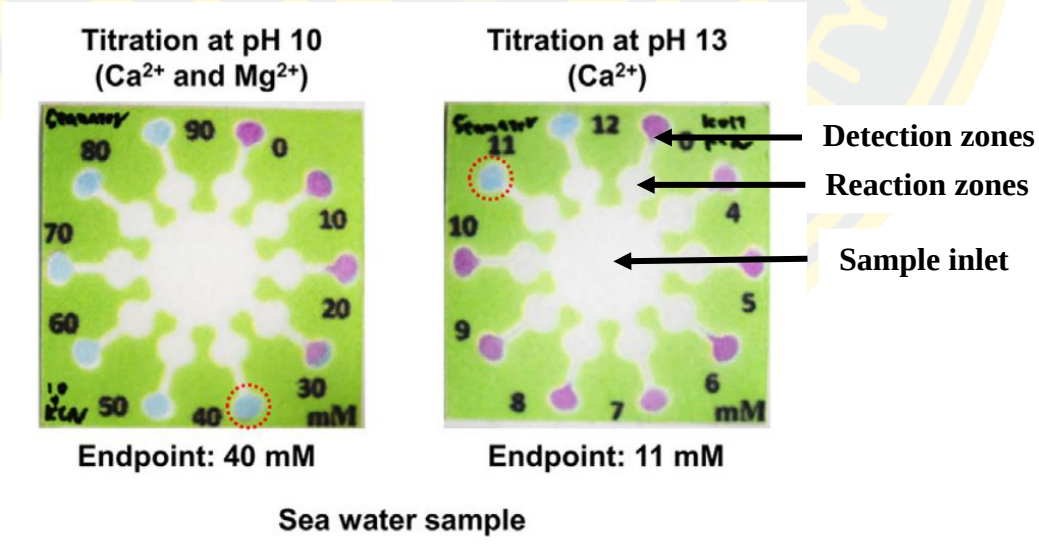

Figures 2-6 Paper-based analytical devices for water hardness using the titration assay. (Karita & Kaneta, 2016)

Shibata, Hiruta, & Citterio, (2019) have developed a paper-based analytical device that allow for the observation of calcium concentration in water by the naked eye, based on the distance at which the color changes. The quantification of calcium ions (Ca^{2+}) is determined through the color change that occurs in the probe cavity. This color change is corrected using an ionophore-doped nano optode, which helps to improve the accuracy of the measurements. The fabrication of the device was based on wax-printing method as shown in Figure 2-7. Once the paper-based devices were prepared, they were filled with the necessary reagents for the calcium concentration analysis. This process resulted in obtaining a functional paper-based device capable of analyzing the calcium concentration in water.

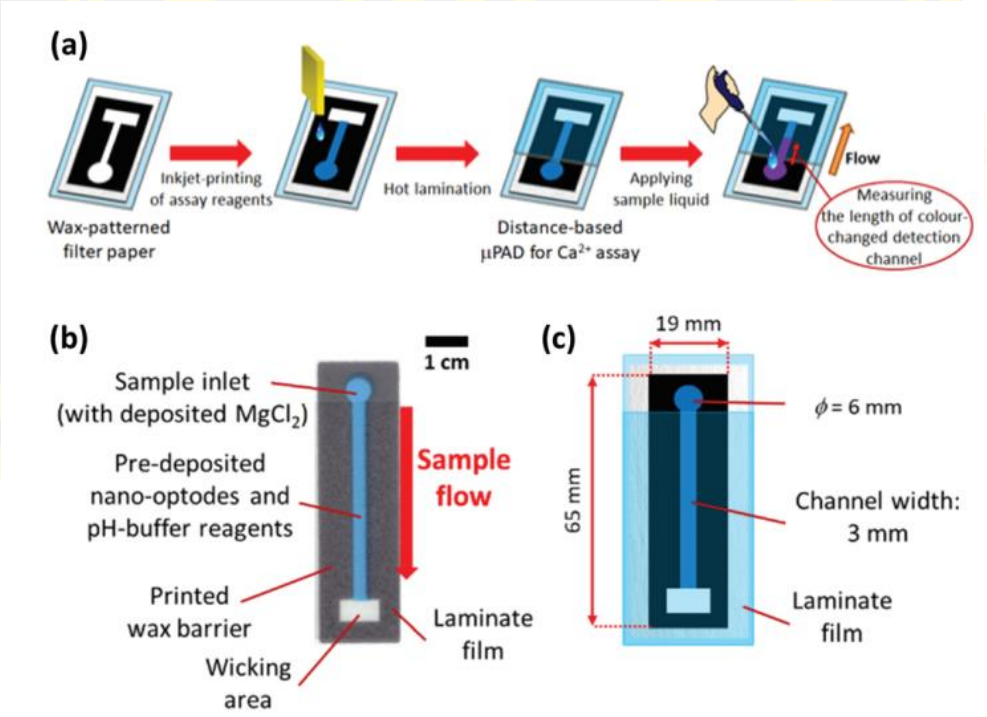

Figures 2-7 (a) Steps of device fabrication with printing technology for Ca^{2+} testing. (b) Distance-based µPAD design for nano optode-based for Ca^{2+} detection. (c) the dimention of the paper-based device. (Shibata, Hiruta, & Citterio, 2019)

In this study, the interfering ions on the Ca^{2+} test was investigated including Na^{+}, K^{+}, Li^{+}, Mg^{2+}, Zn^{2+}, Cu^{2+}, Ni^{2+}, Hg^{2+}, and Al^{3+}. The results shown in Table 3 demonstatred that the developed paper-based device was not significantly affected by the presence of these interfering ions. This indicates that the device specificity for detecting Ca^{2+} was maintained even in the presence of other metal cations at varying concentrations. The study findings suggest that the paper-based device has good selectivity for Ca^{2+} and can provide reliable results for the quantification of calcium concentration in water without being significantly influenced by the presence of other metal ions.

Table 3 Tolerance levels for potentially interfering cations.

Interfering ions	Tolerance [mmol L^{-1}]	Interfering ions	Tolerance [mmol L^{-1}]
Na^{+}	100	Cu^{2+}	1000
K^{+}	100	Ni^{2+}	100
Li^{+}	100	Hg^{2+}	100
Mg^{2+}	100	Al^{3+}	1000
Zn^{2+}	1		

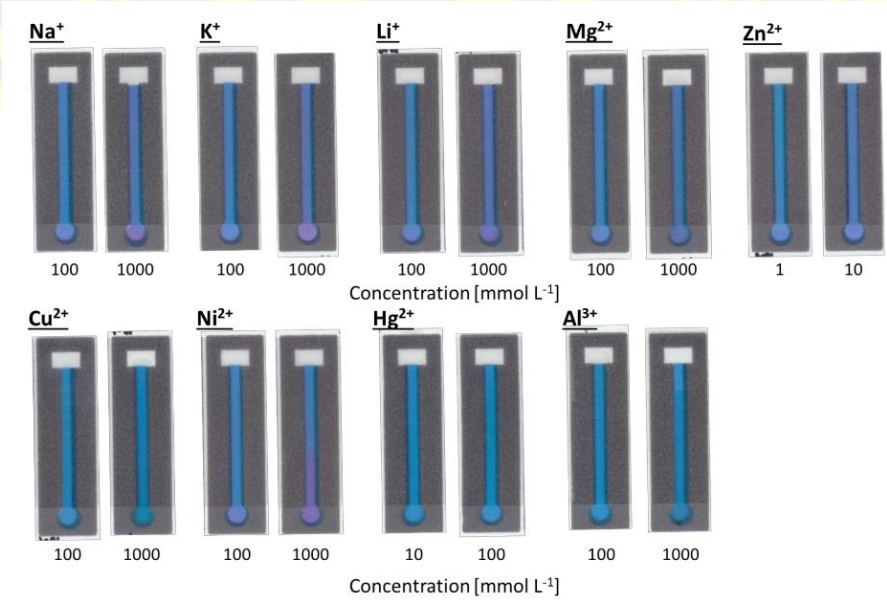

Figures 2-8 Images of a paper-based device obtained from the study of the interfering cations on the analysis of Ca^{2+}. (Shibata et al., 2019)

Rahbar, Paull, & Macka, (2019) developed a paper-based device for the determination of chloride using a distance-based measurement approach based on Mohr's precipitation titration method. The device was constructed using a wax print method and coating on filter paper to create a tube-shaped measuring area connected to the sampling area. The width of the tube was varied to investigate the effect of its shape on the analytical performance. The precipitation reaction between Ag^{+} and $Cr_2O_4^{2-}$ was used in the paper-based device, and the of brown Ag_2CrO_4 precipitate on the tube confirmed the presence of the reagents. When a sample containing Cl^{-} was added to the sampling area, Cl^{-} ions moved along the tube and competed with Ag^{+} ions in the Ag_2CrO_4 precipitate, resulting in the formation of a white precipitate of AgCl. The distance along the tube that appeared white was found to be directly proportional to the Cl^{-} content in the sample, indicating that the device could provide quantitative measurements of chloride. Experimental results showed that the trapezoidal tube shape provided the best detection limit and sensitivity for chloride analysis. The developed paper-based device was compared with the conventional Mohr's precipitation titration method for analyzing chloride in tap water, drinking water, river water, and sweat samples, and the obtained values were not significantly different, indicating the reliable accuracy of the device. The report highlights the advantages of the developed paper-based device, including its portability, affordability, and ease of use. It has the potential for applications in various settings for chloride detection, including environmental monitoring of water sources and analysis of chloride in sweat for physiological studies. Overall, the report suggests that the paper-based device with distance-based measurements has the potential to be a practical and cost-effective method for chloride determination.

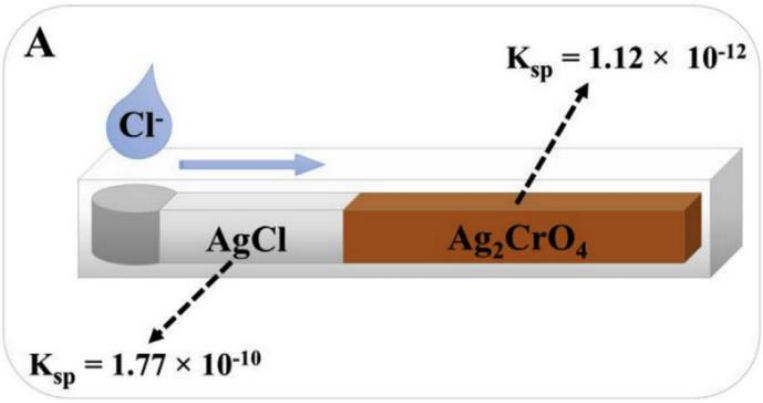

Figures 2-9 Distance-based determination of chloride content on µPADs and solubility of silver chromate versus silver chloride. (Rahbar, Paull, & Macka, 2019)

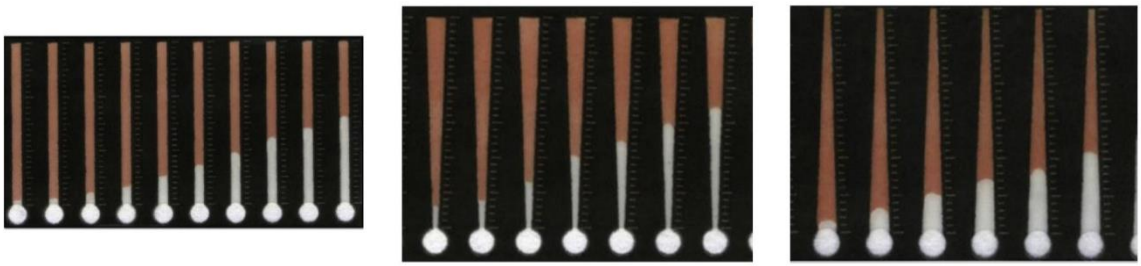

Figures 2-10 The effect of shape designs on the standard chloride detection. (Rahbar et al., 2019)

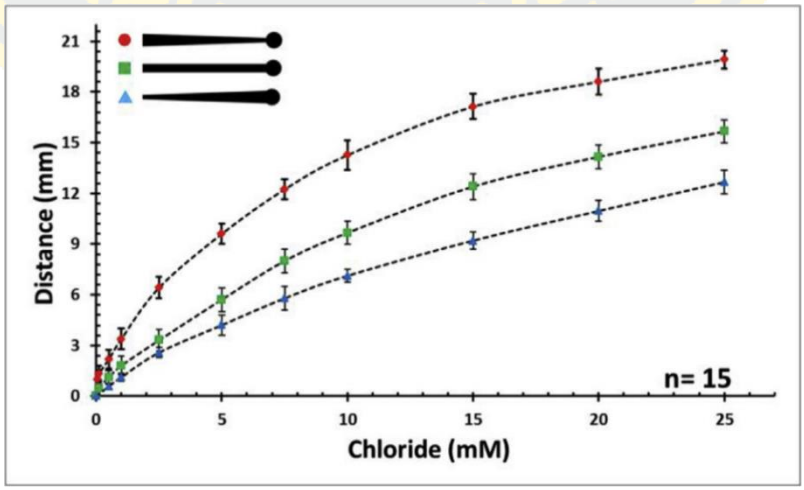

Figures 2-11 Correlation curve between apparent distance-based (mm) and chloride concentration (mM) obtained from chloride measurements with various shape of µPADs. (Rahbar et al., 2019)

Tasangtong et al., (2024) have developed paper sensors for the rapid and user-friendly quantification of chloride using a diameter-based detection format. The analysis relies on the reverse Mohr titration method, where a reddish-brown precipitate of Ag_2CrO_4 is formed and pre-deposited on the circular paper-based test zone. When the sample containing chloride is added to the central sample inlet, chloride flows outward and reacts with Ag_2CrO_4, forming a white precipitate of AgCl. The analysis can be completed within 2–3 min. The diameter of this precipitate is proportional to the chloride concentration in the sample. Diameter signals can be measured using the ImageJ program or a ruler. The developed sensor can analyze real water samples, and its results were compared with those obtained by standard titration methods.

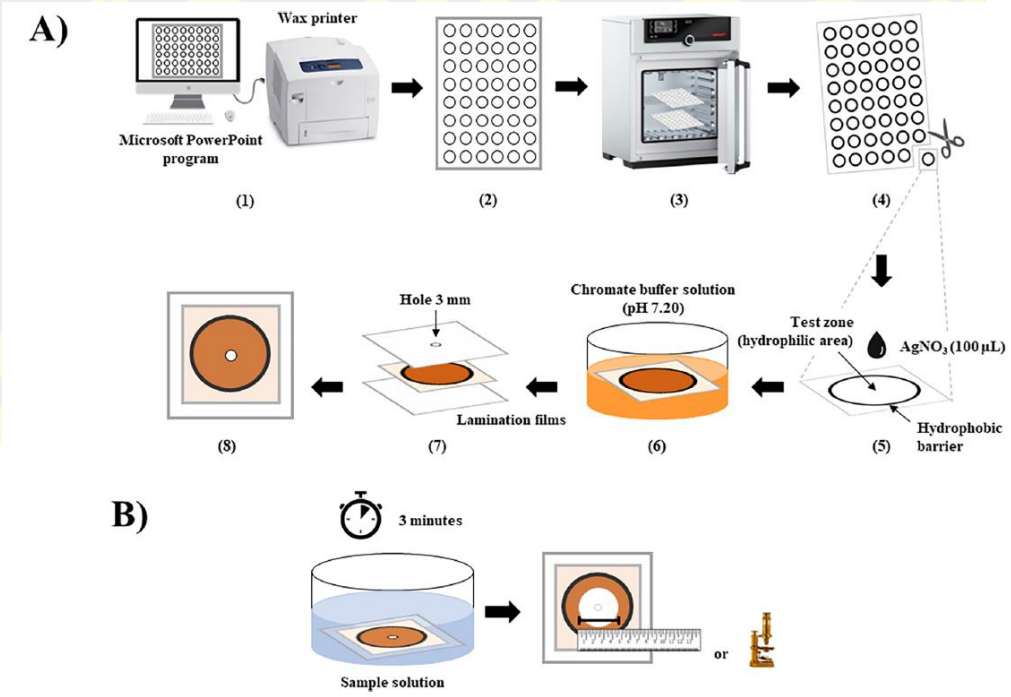

Figures 2-12 Paper-based device for chloride analysis in water. (A) Fabrication of a ready-to-use paper sensor for chloride. (B) Chloride detection procedure using the developed paper sensor. (Tasangtong et al., 2024)

Aryal, Brack, Alexander, & Henry, (2023) have reported developing a multiplexed system by combining a capillary-driven microfluidic device with paper for the simultaneous detection of Ni(II), Fe(III), and Cu(II). The device in this study utilizes origami and lamination techniques to layer the wax-printed 2D paper substrate and its waste zone. It represents the first instance of capillary flow-driven microfluidic devices being used as a transport medium for heavy metal detection. This technique offers rapid assessment of heavy metal exposure in drinking and surface water, significantly reducing assay time.

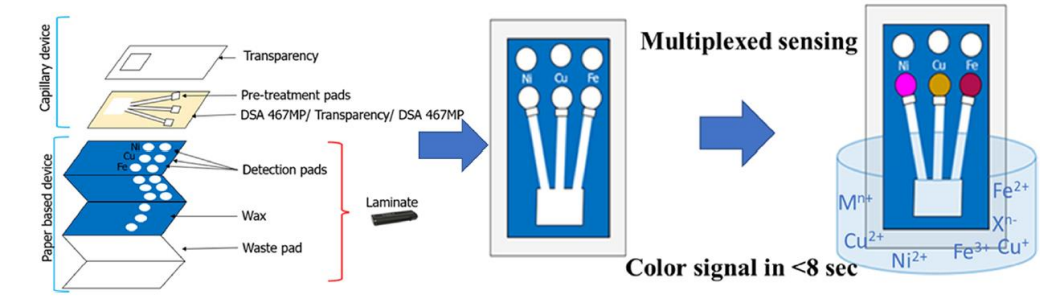

Figures 2-13 Device assembly and operation for simultaneous analysis of heavy metals. (Aryal, Brack, Alexander, & Henry, 2023)

Cate, Noblitt, Volckens, & Henry, (2015) developed a distance-based μPAD was created to simultaneously measure Fe(II), Ni(II), and Cu(II) from aerosolized particulate matter. These metals were selected due to their high prevalence in welding fumes. Typically, metals are extracted from filter samples for chemical speciation. However, this study utilized certified welding fumes in powder form. Hydrophobic barriers and colorimetric reagents were printed to control fluid transport and quantify metals. Reagent deposition via inkjet printing improved assay reproducibility compared to manual deposition. Finally, a certified welding fume standard containing Mn, Fe, Ni, and Zn was utilized to demonstrate the effectiveness of distance-based detection in measuring metal particulates in samples with complex matrices. From the Figures 2-14, it's evident that the multi-channel device can measure Ni, Cu, and Fe simultaneously.

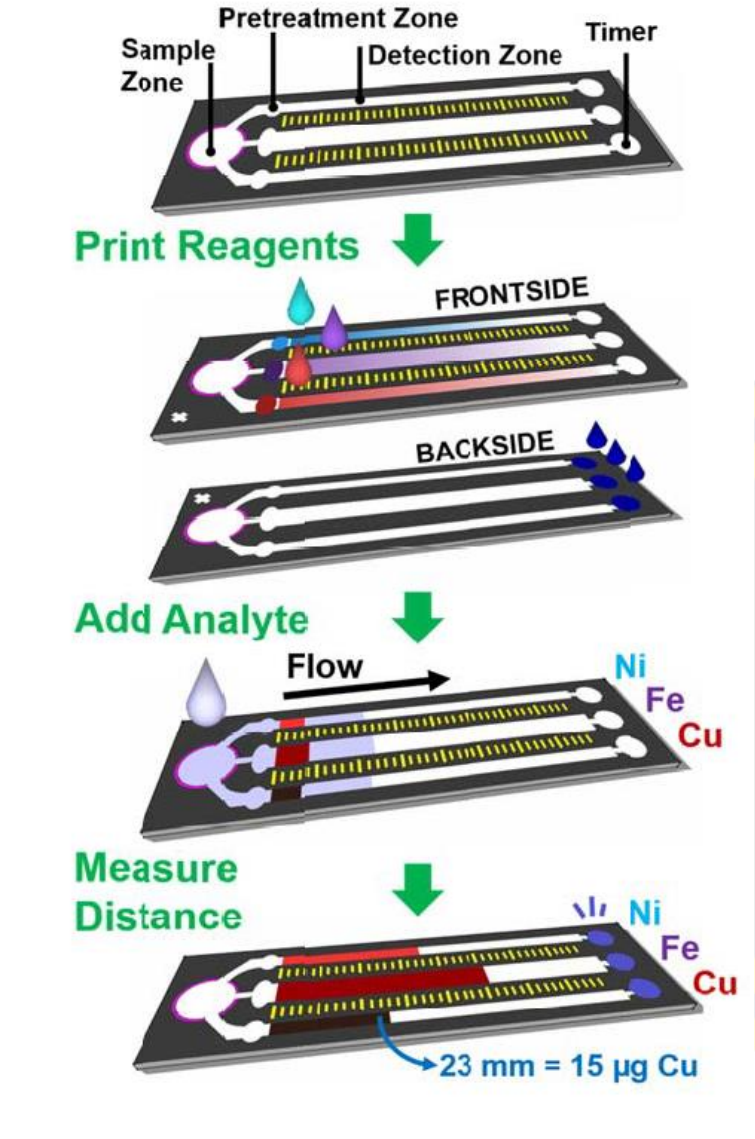

Figures 2-14 Schematic of distance-based detection in multi-layer devices for heavy metals in water. (Cate, Noblitt, Volckens, & Henry, 2015)

CHAPTER 3
METHODOLOGY

3.1 Materials and chemicals

3.1.1 Materials

1. Filter papers no. 1 (Whatman, GE Healthcare company, China)
2. Wax printer (Xerox ColorQube 8870-13, Flextronics Technology, Malaysia)
3. Scanner (Canon CanoScan LiDE110, Canon Inc., Vietnam)
4. Hot Air Oven (1375 FX, Delta laboratory, Thailand)
5. Clear plastic A4 (216 mm. × 303 mm., 100 microns, (One, OfficeMate (Thai) Limited)
6. Laminating machine, (Office pro-LA4P, Olympia Thai, Thailand)
7. Paper punch pliers
8. SpectraMax M2

3.1.2 Chemicals

1. Eriochrome Black T, EBT ($C_{20}H_{12}N_3O_7SNa$), MW: 461.381 g/mol, (Ajax Chemicals, Australia)
2. Glycine ($C_2H_5NO_2$) MW: 75.07 g/mol, CAS: 56-40-6, (Calbiochem®, Germany)
3. N-cyclohexyl-3-aminopropanesulfonic acid, CAPS ($C_9H_{19}NO_3S$), MW: 221.31 g/mol, CAS: 1135-40-6, (Alfa Aesar, Germany)
4. Ammonium Hydroxide 25% Solution (NH_4OH), MW: 35.05 g/mol, CAS: 1336-21-6, (AR grade, RCI Labscan, Thailand)
5. Ammonium Chloride (NH_4Cl_2), MW: 53.49 g/mol, CAS: 12125-02-9, (AR grade, RCI Labscan, Thailand)
6. Methanol (CH_3OH), 99.9% w/w, Density 0.790 g/mL, (AR grade, RCI Labscan, Thailand)
7. Calcium Chloride ($CaCl_2$), MW: 40.078 g/mol, (Ajax Finechem, Australia)

8. Magnesium Chloride ($MgCl_2$), MW: 95.22 g/mol, CAS: 7786-30-3 (Merck KGaA, Germany)

9. Sodium Hydroxide (NaOH), MW: 40 g/mol, CAS: 1310-73-2 (AR grade, Loba Chemie, India)

10. Hydrochloric Acid 37% (HCl), MW: 36.46 g/mol, CAS: 7647-01-0, (AR grade, RCI Labscan, Thailand)

11. Ethylenediaminetetraacetic acid (EDTA), di-sodium salt, dihydrate ($C_{10}H_{14}N_2Na_2O_8 \cdot 2H_2O$), MW: 372.24 g/mol, CAS: 6381-92-6, (AR grade, QRëC® Quality Reagent Chemical, New Zealand)

12. Triethanolamine $N(CH_2CH_2OH)_3$, MW: 149.19 g/mol, CAS: 102-71-6, (KEMAUS, Thailand)

13. Sodium Chloride (NaCl), MW: 58.44 g/mol, CAS: 7647-14-5, (AR grade, Loba Chemie PVT.LTD., India)

14. Lithium Chloride (LiCl), MW: 42.40 g/mol, (APS Ajax Finechem, Australia)

15. Potassium Chloride (KCl), MW: 74.55 g/mol, (Finechem, Australia)

16. Zinc Standard Solution (Zn), 1,000 mg/L, (Loba Chemie, India)

17. Copper Standard Solution (Cu), 1,000 mg/L, (Applichem Panreac, Germany)

18. Nickel Standard Solution (Ni), 1,000 mg/L, (Applichem Panreac, Germany)

19. Mercury (II) Chloride ($HgCl_2$), MW: 271.50 g/mol, CAS: 7487-94-7 (AR grade, QRëC® Quality Reagent Chemical, New Zealand)

20. Aluminum Chloride Hexahydrate ($AlCl_3 \cdot 6H_2O$), MW: 241.45 g/mol, CAS: 7784-13-6, (KEMAUS, Thailand)

21. Silver Nitrate ($AgNO_3$), MW: 169.87 g/mol, CAS: 7761-88-8, (AR grade, QRëC® Quality Reagent Chemical, New Zealand)

22. Potassium Chromate (K_2CrO_4), MW: 194.20 g/mol, CAS: 7789-00-6, (AR grade, Loba Chemie PVT.LTD., India)

23. Potassium Dichromate ($K_2Cr_2O_7$), MW: 294.19 g/mol, CAS: 7778-50-9, (AR grade, QRëC® Quality Reagent Chemical, New Zealand)

24. Sodium Hydrogen Carbonate ($NaHCO_3$), MW: 84.01 g/mol, (APS Finechem, Australia)

25. Calcium carbonate ($CaCO_3$), MW: 100.09 g/mol, (Ajax Finechem, Australia)

26. Iron (II) Chloride Tetrahydrate ($FeCl_2 \cdot 4H_2O$), MW: 198.83 g/mol, CAS: 13478-10-9, (AR grade, QRëC® Quality Reagent Chemical, New Zealand)

27. Iron (III) Chloride Hexahydrate ($FeCl_3 \cdot 6H_2O$), MW: 270.32 g/mol, CAS: 10025-77-1, (AR grade, QRëC® Quality Reagent Chemical, New Zealand)

28. Sodium Fluoride (NaF), MW: 41.99 g/mol, (Ajax Finechem, Australia)

29. Sodium Dihydrogenphosphate ($NaH_2PO_4 \cdot 2H_2O$) MW: 156.01 g/mol, (Ajax Finechem, Austria)

30. Sodium Sulphate Anhydrous (Na_2SO_4), MW: 142.04 g/mol, CAS: 7757-82-6, (Carlo Erba, Italy)

31. Polyethylene Glycol ($HO(C_2H_4O)_nH$; PEG) MW: 6000 g/mol, CAS: 25322-68-3, (Merck KGaA, Germany)

32. Acetic Acid (CH_3COOH), MW: 60.052 g/mol, CAS: 64-19-7, (RCI Labscan,Thailand)

33. Sodium Acetate Anhydrous (CH_3COONa), MW: 82.03 g/mol, CAS: 127-09-3, (AR grade, QRëC® Quality Reagent Chemical, New Zealand)

34. Hydroxylammonium Chloride ($NH_2OH \cdot HCl$), MW: 69.49 g/mol, (Ajax Finechem, Australia)

35. Bathophenanthroline ($C_{24}H_{16}N_2$), MW: 332.41 g/mol, CAS: 1662-01-7, (Tokyo Chemical Industry TCI, Japan)

36. Ethyl Alcohol 99.9% (C_2H_6O), MW: 46.07 g/mol, CAS: 64-1-5, (AR grade, QRëC® Quality Reagent Chemical, New Zealand)

37. Cobalt (II) Chloride ($CoCl_2$), MW: 237.93 g/mol, (Ajax Finechem, Australia)

38. Nitric acid 65% (HNO_3), MW: 63.01 g/mol, (AR grade, QRëC® Quality Reagent Chemical, New Zealand)

39. 1,10-Phenanthroline (Monohydrate) 99.5% ($C_{12}H_8N_2 \cdot H_2O$), MW: 196.23 g/mol, CAS: 5144-89-8, (Loba Chemie, India)

3.1.3 Real Samples

Water samples employed for analysis included tap water, ground water, pond water, system cooling and boiler water and drinking water obtained from locations in north-eastern, and eastern area of Thailand.

3.2 Research plans

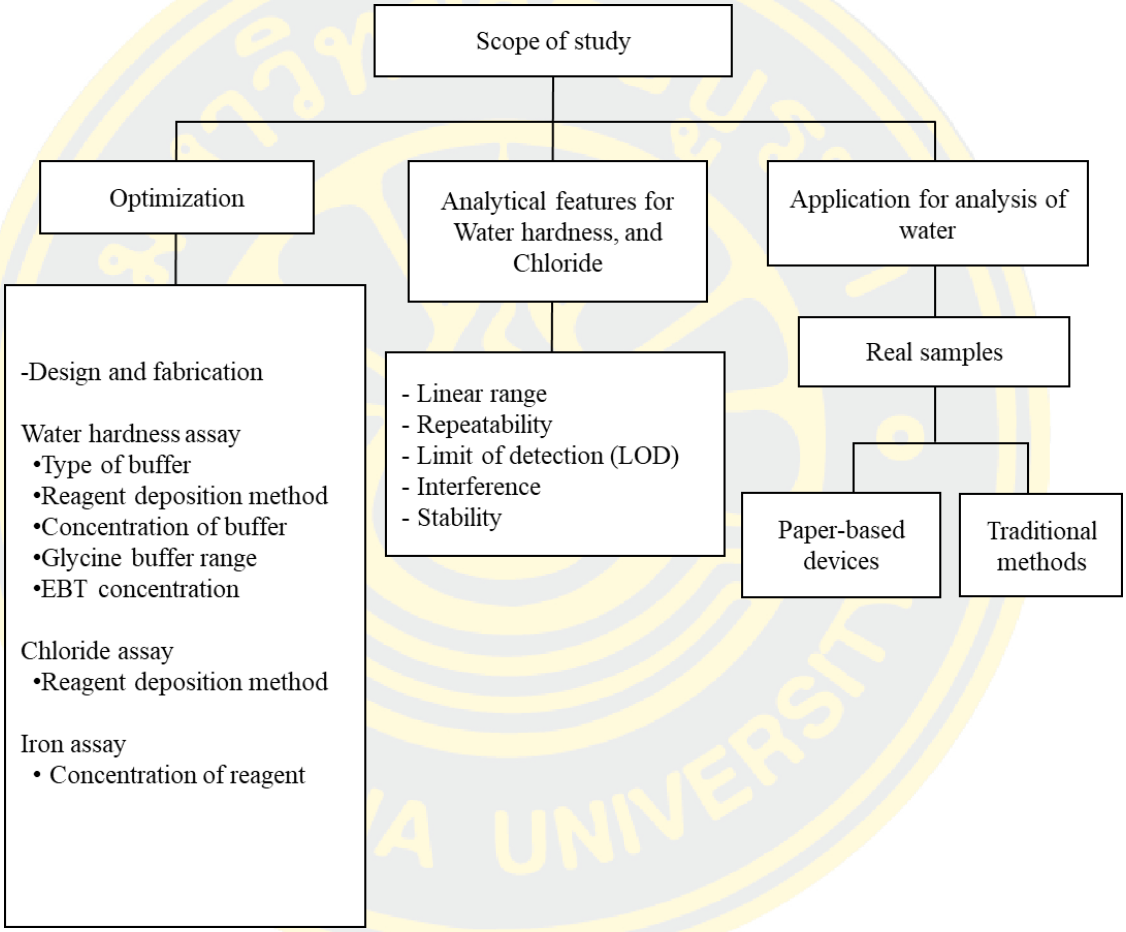

Figures 3-1 Research plans.

3.3 Experimental

3.3.1 Preparation of solution

3.3.1.1 Glycine buffer solution

a) Glycine buffer solution (0.40 M, pH 10)

A 100 mL of glycine buffer solution was prepared by dissolving 3.0050 g in 20 mL of deionized water and mixed with 1.025 g of NaOH dissolved in 20 mL deionized water. The solution mixture was adjusted to 100 mL using deionized water.

b) Glycine buffer solution (0.48 M, pH 10)

A 100 mL of glycine buffer solution was prepared by dissolving 3.6060 g in 20 mL of deionized water and mixed with 1.23 g of NaOH dissolved in 20 mL deionized water. The solution mixture was adjusted to 100 mL using deionized water.

3.3.1.2 CAPS buffer solution (1 M, pH 10)

CAPS buffer solution with the concentration of 1 M was prepared by dissolving 22.1310 g in 100 mL of deionized water.

3.3.1.3 NH_3/NH_4Cl buffer solution

A 100 mL of NH_3/NH_4Cl buffer solution was prepared by dissolving 7.81 g of NH_4Cl in 10 mL of deionized water and adding NH_4OH 56.4 mL The solution mixture was adjusted to 100 mL using deionized water. The final pH of the solutions was adjusted to 10 with NaOH or HCl solution.

3.3.1.4 Eriochrome Black T (EBT) solution

Stock solution of 5 mM EBT 50 mL was prepared by dissolving 0.1150 g of EBT in 10 mL of methanol and adjusting the volume to 10 mL with deionized water.

3.3.1.5 Magnesium chloride ($MgCl_2$) solution

Stock solution of magnesium 50 mM was prepared by dissolving 0.2385 g of $MgCl_2$ in 50 mL of deionized water.

3.3.1.6 Calcium chloride ($CaCl_2$) solution

Stock calcium solution with the concentration of 50 mM was prepared by dissolving 0.2788 g of $CaCl_2$ in 50 mL of deionized water.

3.3.1.7 Sodium Hydroxide (NaOH) solution

Sodium Hydroxide solution with the concentration of 1 M was prepared by dissolving 4.00 g in 100 mL of deionized water.

3.3.1.8 Hydrochloric Acid (HCl) solution

Stock Hydrochloric Acid solution (12 M) was diluted to concentrations of 1 M with deionized water.

3.3.1.9 Sodium chloride (NaCl) solution

Stock sodium chloride solution (60 mM) was prepared by dissolving 0.0880 g of NaCl in 25 mL of deionized water.

3.3.1.10 Potassium Chloride (KCl) solution

Stock potassium chloride solution (60 mM) was prepared by dissolving 0.1120 g of KCl in 25 mL of deionized water.

3.3.1.11 Lithium chloride (LiCl) solution

Stock lithium chloride solution (60 mM) was prepared by dissolving 0.0640 g of LiCl in 25 mL of deionized water.

3.3.1.12 Mercury (II) chloride ($HgCl_2$) solution

Stock mercury chloride solution (60 mM) was prepared by dissolving 0.4100 g of $HgCl_2$ dissolved in 25 mL of acetic buffer pH 5.

3.3.1.13 Aluminum chloride hexahydrate solution

Stock aluminum chloride solution (60 mM) was prepared by dissolving 0.3620 g of $AlCl_3$ in 25 mL of deionized water.

3.3.1.14 Zinc chloride ($ZnCl_2$) solution

Stock zinc chloride solution (60 mM) was prepared by dissolving 0.2050 g of $ZnCl_2$ in 25 mL of deionized water.

3.3.1.15 Copper (Cu) solution

Stock copper solution (15.737 mM) was diluted to concentrations of 1 mM with deionized water.

3.3.1.16 Nickel (Ni) solution

Stock nickel solution (17.038 mM) was diluted to concentrations of 1 mM with deionized water.

3.3.1.17 EDTA solution

EDTA solution with a concentration of 0.005 M was prepared by dissolving 0.47 g in 250 mL of deionized water.

3.3.1.18 Eriochrome Black T (EBT) indicator solution

Eriochrome Black T (EBT) indicator solution was prepared by dissolving 100 mg in a solution containing 15 mL of triethanolamine and 5 mL of methanol.

3.3.1.19 Silver nitrate ($AgNO_3$) solution

a) Silver nitrate solution (0.01 M)

Stock silver nitrate solution (0.01 M) was prepared by dissolving 0.8495 g of $AgNO_3$ in 500 mL of deionized water.

b) Silver nitrate solution (12.5 mM)

Stock silver nitrate solution (12.5 mM) was prepared by dissolving 0.1062 g of $AgNO_3$ in 50 mL of deionized water.

c) Silver nitrate solution (50 mM)

Stock silver nitrate solution (50 mM) was prepared by dissolving 0.4247 g of $AgNO_3$ in 50 mL of deionized water.

3.3.1.20 Chromate ($Cr_2O_4^{2-}$) solution

a) Chromate solution (50 mM)

Chromate solution (50 mM, pH 7.20) was prepared by dissolving 0.1 g of potassium chromate in deionized water and mixed with 0.8350 g of potassium dichromate dissolved in deionized water. The solution mixture was made up to the final volume of 100 mL with deionized water. The final pH of the solutions was adjusted to 7.20 with NaOH or HCl solution.

b) Chromate solution (100 mM)

Chromate solution (100 mM, pH 7.20) was prepared by dissolving 0.20 g of potassium chromate in deionized water and mixed with 1.67 g of potassium dichromate dissolved in deionized water. The solution mixture was made up to the final volume of 100 mL with deionized water. The final pH of the solutions was adjusted to 7.20 with NaOH or HCl solution.

3.3.1.21 Sodium chloride (NaCl) solution

Stock sodium chloride solution (250 mM) was prepared by dissolving 14.61 g of NaCl in 1000 mL of deionized water.

3.3.1.22 Sodium Hydrogen Carbonate ($NaHCO_3$) solution

Sodium Hydrogen Carbonate solution (2%) was prepared by dissolving 10 g in 500 mL of deionized water.

3.3.1.23 Potassium Chromate (K_2CrO_4) indicator solution

Potassium Chromate indicator solution (2.5%) was prepared by dissolving 2.5 g in 100 mL of deionized water.

3.3.1.24 Iron (Fe^{2+}) solution

a) Iron solution (1,000 mg/L)

Stock iron solution (1,000 mg/L) was prepared by dissolving 0.3560 g of Fe^{2+} in 100 mL of deionized water at pH 4.5.

b) Iron solution (10 mM)

Stock iron solution (10 mM) was prepared by dissolving 0.0994 g of Fe^{2+} in 50 mL of deionized water at pH 4.5.

3.3.1.25 Iron (Fe^{3+}) solution

Stock iron solution (10 mM) was prepared by dissolving 0.1352 g of Fe^{3+} in 50 mL of deionized water at pH 4.5.

3.3.1.26 Fluoride (F^-) solution

Stock fluoride solution (50 mM) was prepared by dissolving 0.1050 g of NaF in 50 mL of deionized water.

3.3.1.27 Phosphate (PO_4^{3-}) solution

a) Phosphate solution (1,000 mg/L)

Stock phosphate solution (1,000 mg/L) was prepared by dissolving 16.4 mg of PO_4^{3-} in 10 mL of deionized water.

b) Phosphate solution (50 mM)

Stock phosphate solution (50 mM) was prepared by dissolving 0.3900 g of PO_4^{3-} in 50 mL of deionized water.

3.3.1.28 Sulfate (SO_4^{2-}) solution

a) Sulfate solution (1,000 mg/L)

Stock sulfate solution (1,000 mg/L) was prepared by dissolving 14 mg of SO_4^{2-} in 10 mL of deionized water.

b) Sulfate solution (50 mM)

Stock sulfate solution (50 mM) was prepared by dissolving 0.3551 g of SO_4^{2-} in 50 mL of deionized water.

3.3.1.29 Bicarbonate (HCO_3^-) solution

a) Bicarbonate solution (1,000 mg/L)

Stock bicarbonate solution (1,000 mg/L) was prepared by dissolving 13.8 mg of HCO_3^- in 10 mL of deionized water.

b) Bicarbonate solution (50 mM)

Stock bicarbonate solution (50 mM) was prepared by dissolving 0.2100 g of HCO_3^- in 50 mL of deionized water.

3.3.1.30 Polyethylene Glycol (PEG) solution

Polyethylene Glycol solution (1%) was prepared by dissolving 1 g in 100 mL of deionized water.

3.3.1.30 Acetate buffer solution (1 M, pH 4.5)

(a) Stock acetate acid solution (16.6 M) was diluted to concentrations of 1 M in 100 mL of deionized water. (b) Sodium acetate solution with a concentration of 1 M was prepared by dissolving 8.203 g in 100 mL of deionized water. A 100 mL acetate buffer solution was prepared by mixing 31 mL of 1 M acetate acid solution with 20 mL of 1 M sodium acetate solution. The solution mixture was adjust to 100 mL using deionized water. The final pH of the solutions was adjusted to 4.5 with NaOH or HCl solution.

3.3.1.31 Hydroxylamine solution

Hydroxylamine solution (10%) was prepared by dissolving 2.5 g in 25 mL of acetate buffer solution (1 M, pH 4.5).

3.3.1.32 Bathophenanthroline (Bphen) solution

Bphen solution with a concentration of 1 mM was prepared by dissolving 8.31 mg in 25 mL of Ethanol 99.9% solvent.

3.3.1.33 Cobalt (Co^{2+}) solution

Stock cobalt solution (1,000 mg/L) was prepared by dissolving 0.0404 g of Co^{2+} in 10 mL of deionized water.

3.3.2 General procedure for device fabrication and simultaneous detection of water hardness, chloride and iron in water

3.3.2.1 General procedure of the paper-based device fabrication

The paper-based sensor was fabricated using the following steps. Firstly, the device was initially created using Microsoft PowerPoint with a circle of 3 cm diameter. The design was transferred to the Whatman Grade 1 filter paper using a wax printer. The pattern paper was heated to melt wax into paper to create a hydrophobic barrier. Then, the reagents were loaded on the detection zones. The device's detection zones was coated with specific reagents to detect each analyte. Finally, the device was coated by lamination films and a 3-mm hole of the top film was drilled in the center of the paper-based device for use as sample inlet. Then, the paper-based device for water analysis was obtained.

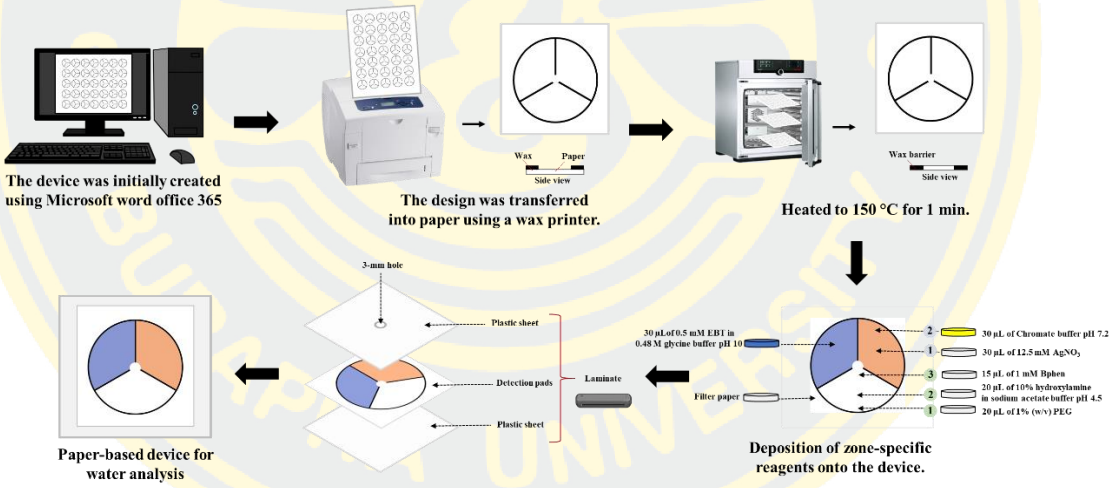

Figures 3-2 The fabrication paper-based device fabrication for simultaneous analysis.

3.3.2.2 General procedure for simultaneous analysis of water hardness and chloride in water using the developed paper-based device.

For the detection process, the analysis of water was performed by adding 75 µL standard/sample solution into the sample inlet to allow flow from the center outward radially to the circumference. After 3 min, the radial distance of the color band developed was measured with a ruler or Image J program and used to quantify water hardness, chloride and iron in water, as shown in Figure 3-3.

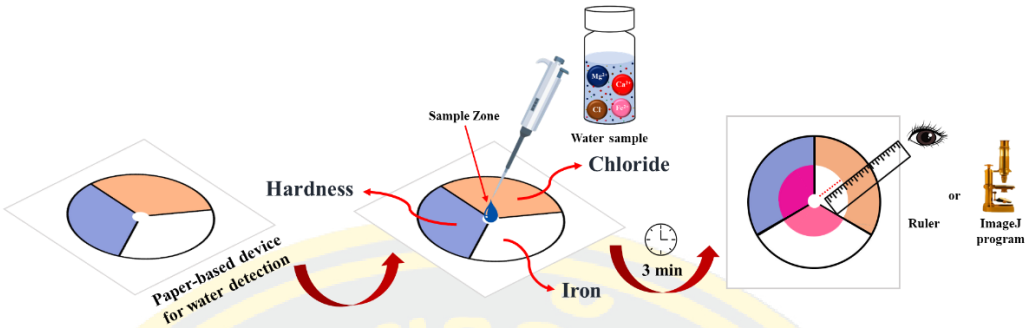

Figures 3-3 The measurement procedure for water quality assessment using microfluidic paper-based analytical device (μPAD) with radial distance-based measurement.

3.3.3 Design and fabrication of paper-based devices

3.3.3.1 Design of paper-based device for a single analysis

The paper-based device was fabricated using wax-printing technique. It was designed to have in the shape of a circle with a diameter of 3 cm. (Figure 3-4) using Microsoft Word Office 365. The design was printed on filter paper No. 1 using a wax printer (Xerox ColorQube 8870-13) and heated to 150 °C in an incubator for 1 minute to create a hydrophobic barrier. The transparent tape was adhered to the back of the filter paper device to prevent leakage.

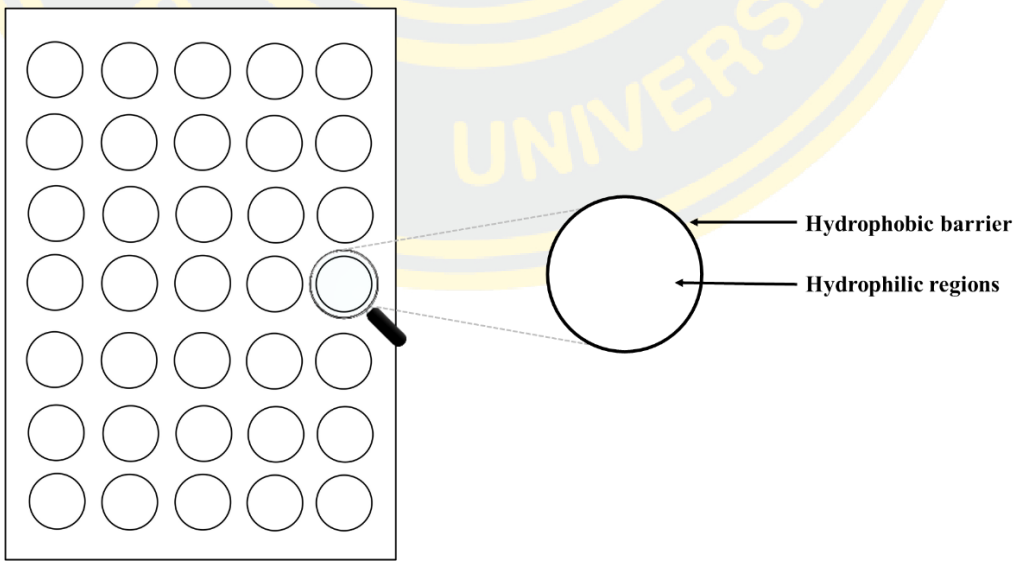

Figures 3-4 The paper-based devices for single analyte analysis designed by the Microsoft word office 365 program.

3.3.3.2 Design of paper-based device for a simultaneous analysis

A paper-based device was designed to have a circle shape with a diameter of 3 cm. The circle consists of 3 sections for 3-analyte analysis at the same time (Figure 3-5). The device was fabricated using wax-printing technique where the process is described above.

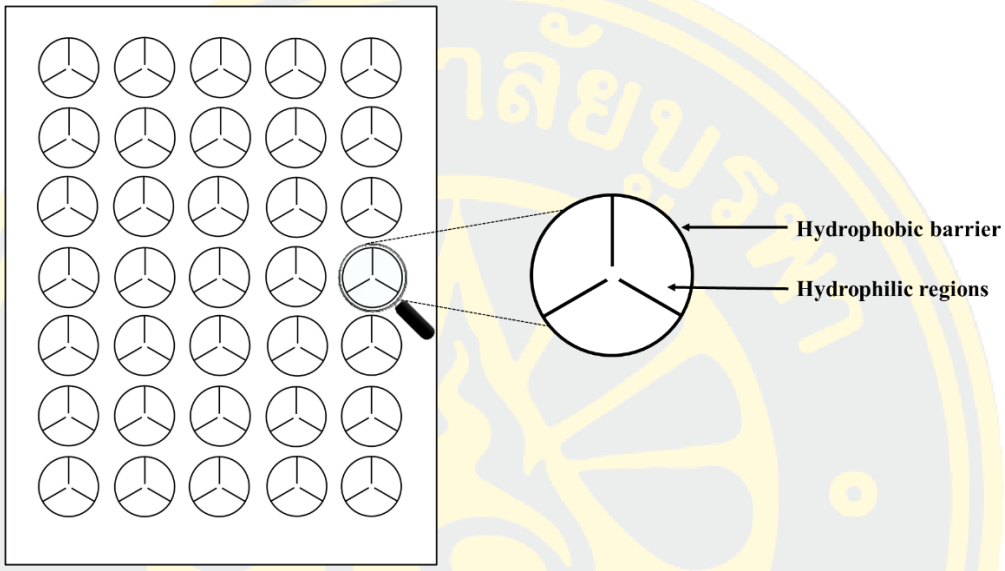

Figures 3-5 The paper-based devices for simultaneous analysis.

3.3.4 Optimization

3.3.4.1 Water hardness assay

a) Type of buffer

Water hardness analysis relies on the reaction between calcium and magnesium ions and EBT ligand, which is typically performed at a pH of 10. To ensure the reaction takes place at pH 10, the appropriate type of buffer must be utilized. Typically, ammonium buffer is employed for this purpose. However, ammonium buffer tends to evaporate easily, making it unsuitable for the preparation of ready-to-use tests that require an extended shelf life. Here, two buffer systems were evaluated including glycine and CAPS buffers with pKa of 9.78 and 10.4, respectively.

b) Reagent deposition method for single-analyte analysis system: Two-step reagent deposition

The two-step reagent deposition process on paper-based devices is shown in Figure 3-6. Firstly, 75 µL of glycine buffer or CAPS buffer pH 10 was placed on paper at the test area and dried at 35 °C for 10 min. Then, 150 µL of 0.5 mM EBT solution was added and dried at 35 °C for 30 min. Finally, a paper-based device for water hardness analysis was obtained.

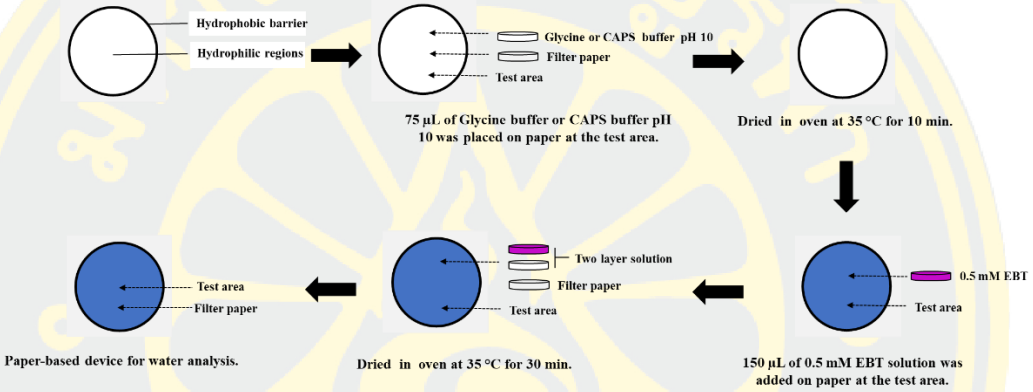

Figures 3-6 Two-step reagent deposition process on a paper-based device for water hardness analysis (Two layers, without lamination plastic).

The effect of lamination process was also studied by laminating the paper-based device prepared by two-step reagent deposition process prior to water hardness analysis. The obtained paper-based device was sandwiched with clear plastic films and laminated using thermal lamination method. A 3-mm hole was drilled in the center of the top plastic film for use as a sample inlet.

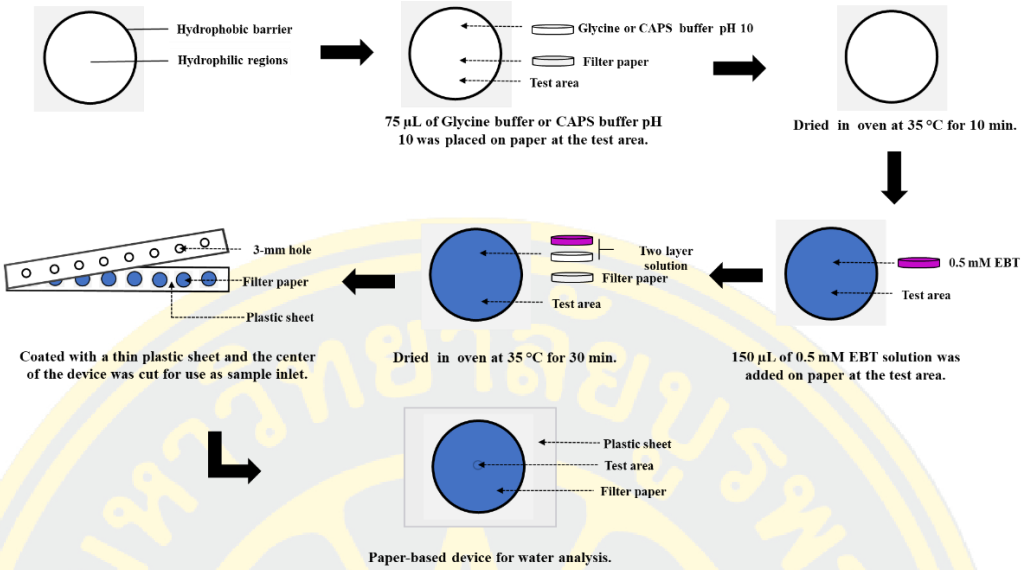

Figures 3-7 The lamination method for a paper-based device deposited by two-step reagents.

c) Reagent deposition method for single-analyte analysis system: One-step reagent deposition

The one-step reagent deposition process of a paper-based device is shown in Figure 3-8. A 150 µL of a solution mixture of 0.5 mM EBT in Glycine buffer or CAPS buffer pH 10 was loaded onto the test zone of a paper-based device and allowed to dry at 35 °C for 30 min. Finally, a paper-based device for water hardness analysis was obtained.

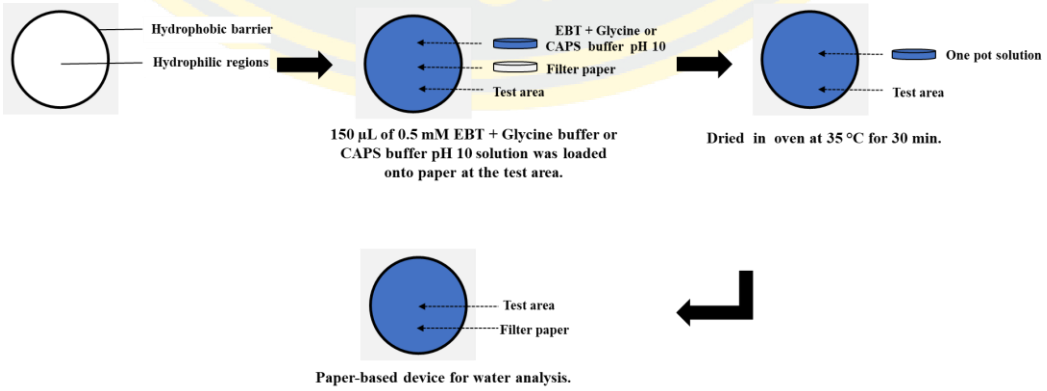

Figures 3-8 Schematic diagram showing the fabrication of a paper-based device for water hardness analysis (One-step, without lamination plastic).

To investigate the impact of the lamination process, the paper-based devices prepared by the one-step reagent deposition process was laminated and investigated for its efficiency for water hardness analysis compared to those that were not.

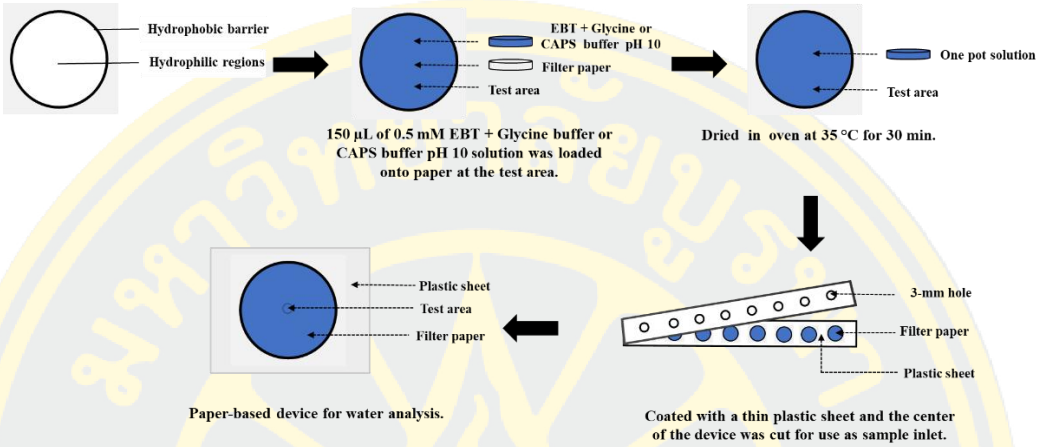

Figures 3-9 Schematic diagram showing the fabrication of a paper-based device for water hardness analysis (One-step, lamination plastic).

d) Reagent deposition method for simultaneous analysis: Dropping

Dropping method for reagent deposition was shown in Figure 3-10. For water hardness analysis, the 150 µL solution mixture of 0.5 mM EBT in Glycine buffer pH 10 was dropped at the center of the devices and allowed to flow radially to cover the entire test zone. The device was then dried at 35 °C for 30 min before being laminated. For lamination, the paper-based device was placed between two films, with a 3-mm hole drilled at the center of the top film to serve as a sample inlet. Finally, a paper-based device for water hardness analysis was obtained.

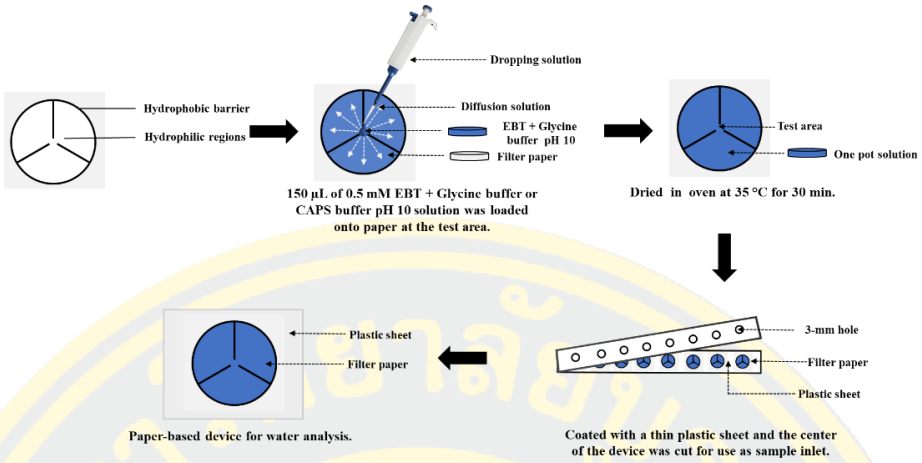

Figures 3-10 Schematic diagram showing fabrication a paper-based device for water hardness analysis by dropping the solution into the paper-based device (One-step, lamination plastic).

e) Reagent deposition method for simultaneous analysis: Dipping

The process of dipping the solution into the paper-based device is shown in Figure 3-11. 0.5 mM EBT + Glycine buffer pH 10 solution was prepared in a plate, then a paper-based device was dipping into the solution for 20 s, and then dried at 35. °C for 30 min for the solution to dry. Then coated with clear plastic using a laminator. where the top plastic sheet drilled a 3-mm hole for inserting the sample. Finally, a paper-based device for water hardness analysis was obtained.

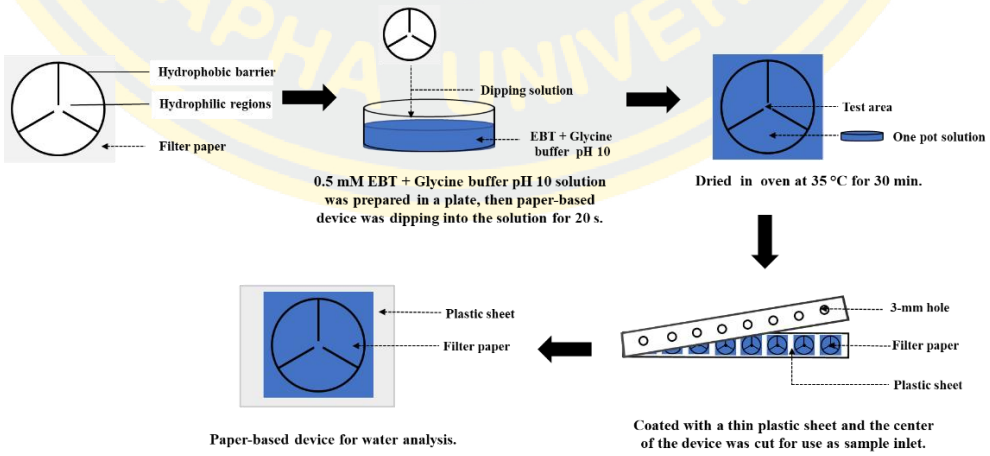

Figures 3-11 Schematic diagram showing fabrication a paper-based device for water hardness analysis by dipping the solution into the paper-based device (One-step, lamination plastic).

f) Concentration of buffer

Glycine buffer solution was prepared at pH 10 with concentrations of 0.40 M and 0.48 M. These solutions were used to dilute the stock EBT solution (5 mM) to achieve a final EBT concentration of 0.5 mM. The solution was appied onto the test area of the device and dried at 35°C for 30 minutes. A mixture of Ca^{2+}/Mg^{2+} solution was added onto the paper device, allowing the standard solution to flow until the test area was completely filled. The paper-based device changes color from blue to magenta upon adding the standard solution.

g) Glycine buffer range

Glycine buffer solution was prepared at pH 8-10 with a concentration of 0.48 M. The pH was adjusted to 8-10 with NaOH or HCl solution. The solution was employed to test its effect on water hardness detection in similar manner to that of buffer concentration study described above.

h) EBT concentration

EBT solutions at concentrations of 0.1, 0.5, 1 and 2 mM were prepared in Glycine buffer pH 10 and investigated for its effect on the assay sensitivity. The prepared solution was deposited on the paper-based devices and the devices were further fabricated by the process described above. The devices were then used to detect water hardness where different concentrations of calcium ions were employed for this study.

3.3.4.2 Chloride assay

a) Reagent deposition method

The methods for deposition of $Cr_2O_4^{2-}$ solution onto paper-based devices was evaluated including multiple dropping method, single dropping method and dipping method. The apparent diameter of color from the analysis of chloride was observed to determine optimal deposition method for $Cr_2O_4^{2-}$ solution.

3.3.4.3 Iron assay

a) Concentration of reagent

Firstly, 1% (w/v) PEG was loaded onto the test zone for iron assay and allowed to dry. Next, 10% (w/v) hydroxylamine was prepared in acetate buffer (1 M, pH 4.5). Finally, Bphen solutions at concentrations of 0.25, 0.5, 1.0, 2.5, 5, 10 and 20 mM were prepared in Ethanol 99.9% solvent. The prepared solution was deposited on the paper-based devices and the devices were further fabricated by the process described above. The devices were then used to detect iron in water where different concentrations of iron ions were employed for this study.

3.3.5 Analytical features

3.3.5.1 Linear range

a) Water hardness assay

The paper-based devices prepared under optimal conditions were employed for the detection of calcium ions used as water hardness standards with a concentration of 13-4003 mg/L. A graph of color radial distance was plotted as a function of calcium concentration (n=6) to determine the linearity of the water hardness in term of calcium carbonate.

b) Chloride assay

The paper-based devices prepared under optimal conditions were employed for the detection of chloride standard solutions with a concentration range of 0.25 - 100 mM. A graph of color diameter was plotted as a function of chloride concentration (n=6) to determine the linearity of chloride analysis.

c) Iron assay

The paper-based devices prepared under optimal conditions were employed for the detection of iron standard solutions with a concentration range of 0.5-300 mg/L. A graph of color diameter was plotted as a function of iron concentration (n=3) to determine the linearity of iron analysis.

3.3.5.2 Repeatability

The repeatability of the developed method was assessed by conducting six replicate analyses for water hardness and chloride, and three replicate analyses for iron with concentrations within the linear range of the analyte standard. The relative standard deviation was then calculated to determine method repeatability.

3.3.5.3 Limit of detection (LOD)

The blank solution (n=10) was measured and the standard deviation was determined to calculate the LOD using the following formula.

$$\text{LOD} = \frac{3\text{SD}}{\text{Slope}} \qquad \text{Equation 3.1}$$

3.3.6 Interference Studies

For water hardness assay, interfering metals including Na^{+}, K^{+}, Li^{+}, Zn^{2+}, Cu^{2+}, Ni2+, Hg^{2+} and Al^{3+}were investigated for its effect on water hardness analysis. Each ion was added to the 1 mM calcium standard solution.

For chloride assay, ions including Fe^{2+}, Fe^{3+}, Zn^{2+}, Cu^{2+}, F^{-}, PO_4^{2-}, SO_4^{2-} and HCO_3^{-} were investigated for its effect on Cl^{-} analysis. Each ion was added to the 1 mM Cl^{-} standard solution.

For iron assay, ions including Zn^{2+}, Cu^{2+}, Co^{2+}, Mg^{2+}, Ni^{2+}, PO_4^{2-}, SO_4^{2-} and HCO_3^{-} were investigated for its effect on Fe^{2+} analysis. Each ion was added to the 1 mg/L Fe^{2+} standard solution.

The signal of the test was then measured on the paper-based device to determine effect of each ion on analysis of water hardness, chloride, and iron in water.

3.3.7 Storage Stability Study

The paper-based device stability was investigated over two months under different storage conditions. All devices were prepared at the same time, kept in Mylar and Ziplock bags and stored at room temperature (25-38°C, RT Dark) and in the fridge at 6-10°C. Stability tests were conducted every five days. For water hardness, a 1.5 mM standard solution containing an equal ratio of Ca^{2+} and Mg^{2+} was used to test. For chloride, standard solution at a concentration of 7 mM was employed to test chloride devices and Fe^{2+} standard solution at a concentration of 1 mg/L was employed to test the stability of iron detection zones. The results were compared to those obtained from the tests using the freshly prepared devices.

3.3.8 Sample analysis

Samples used for analysis included tap water, pond water, groundwater, system cooling and boiler water were collected at different sites including from industry sector, rural and urban areas of Thailand. Tap water and groundwater were analyzed without further sample preparation. Pond water, system cooling and boiler water was prepared by filtering the samples using Whatman No. 1 filter paper before analysis. For iron analysis, the pH of all samples was adjusted to 4.5 using nitric acid (HNO_3) before analysis.

3.3.9 Diameter measurement analysis with ImageJ software

1. Open the ImageJ program, click on the File menu and Open, and select the image to be analyzed.

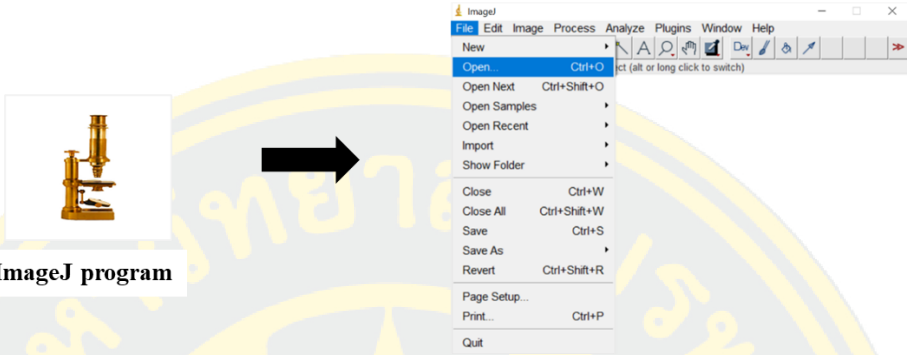

2. Set the diameter measurement by pressing Analyze and selecting the menu Set Scale. A bar will appear to select the setting as shown in the image below and press OK.

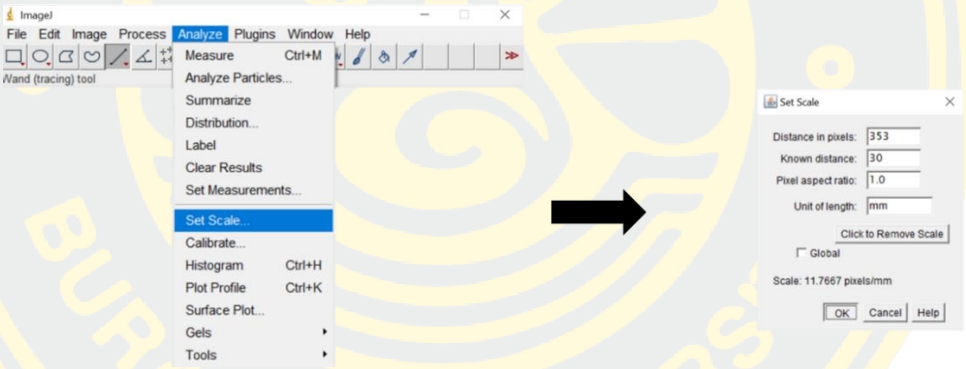

3. Select the area that you want to measure the diameter (Diameter) by selecting from the desired diameter, then press Ctrl+M or M. The Length value obtained from the image processing in the selected area.

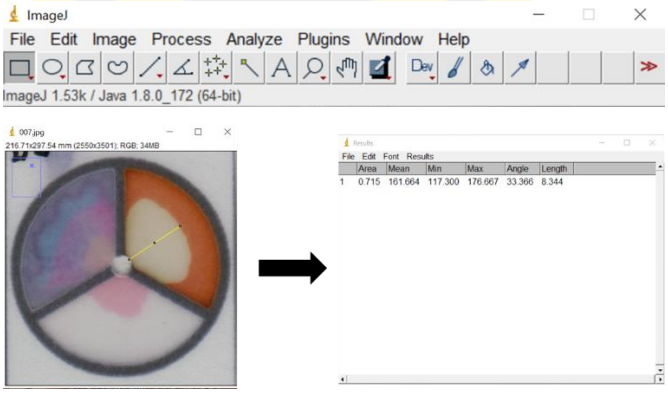

3.3.10 Traditional titration method for water hardness and chloride analysis.

Traditional methods for water hardness analysis typically involve titration techniques. One common method is EDTA titration, where ethylenediaminetetraacetic acid (EDTA) is used as a titrant and added to the water sample containing Ca^{2+}/Mg^{2+} that is added by EBT to form Ca/Mg-EBT red complex. EDTA reacts with calcium and magnesium ions in the water, forming stable complexes leaving the free EBT with blue color at the endpoint of titration. This reaction is indicated by a color change, allowing the determination of water hardness. (© The Open University, 2019)

Chloride analysis was measured traditionally using Mohr's Method. This method is commonly used in titrations for chloride with silver nitrate ($AgNO_3$) standard solutions. By adding chromate ion (CrO_4^{2-}), an indicator, to the neutral chloride sample solution initiates the process. Titration with a standard silver nitrate solution triggers the formation of silver chloride (AgCl) precipitate initially. Once the silver chloride precipitate fully forms, subsequent addition of silver nitrate leads to the formation of a reddish-brown precipitate of silver chromate (Ag_2CrO_4). Silver chromate is more soluble than silver chloride, facilitating clearer observations. (University of Canterbury)

Spectrophotometry was traditionally employed for determination of iron (II) content. An orange-red complex forms between the Fe (II) ion and 1,10-phenanthroline was formed. Complex formation occurs regardless of the solutions pH, but it's typically conducted at around pH 3.5 to avoid iron salt precipitation. Absorbance is then measured at a wavelength of 510 nm. (Harvey Jr, 1955)

CHAPTER 4
RESULTS AND DISCUSSION

4.1 The principle of the proposed assay

The water hardness test relies on the reaction between calcium and magnesium complexes with EBT loaded onto a paper-based device featuring a test zone. As shown in the equation in Figure 4-1, the color radial distance is determined by the concentration of both types of ions in the sample, allowing for the analysis of water hardness.

$$\text{EBT} + M^{2+} \xrightarrow{\text{pH = 10}} \text{[M-EBT] complex}$$

Magenta color

Figures 4-1 The complex reaction between EBT and Ca^{2+}, Mg^{2+}.

For chloride test, the paper-based device utilizes the precipitation reaction of Cl^- with Ag^+ in the Ag_2CrO_4 precipitate within the test zone. Chloride test in water was carried out by adding the desired sample to the loading area. The Cl^- solution spread to the device's edge, reacting with Ag_2CrO_4, causing the paper to change color from brown to white. As shown in the equation in Figure 4-2, the color radial distance depends on the Cl^- concentration in the sample. Chloride content was analyzed by measuring the radial distance using the ImageJ program or a ruler.

$$2Ag^+ (aq) + CrO_4^{2-} (aq) \rightleftharpoons Ag_2CrO_4 (s) \quad (1)$$

$$Ag_2CrO_4(s) + 2Cl^- (aq) \rightleftharpoons 2AgCl (s) + CrO_4^{2+}(aq) \quad (2)$$

(Reddish-brown precipitate) (White precipitate)

Figures 4-2 The precipitation reaction of silver chromate with chloride.

In the iron test, Bathophenanthroline reacts with Fe^{2+} under acidic conditions (pH 4.5) on a paper device within the test zone. When the desired sample is dropped into the sample loading area, the Fe^{2+} solution spreads to the edge of the device. Bathophenanthroline reacts with Fe^{2+}, causing the change from white to a red complex. The color radial distance observed in the reaction (Figure 4-3) corresponds to the Fe^{2+} concentration in the sample. Fe^{2+} analysis is conducted by measuring the radial distance using the ImageJ program or a ruler.

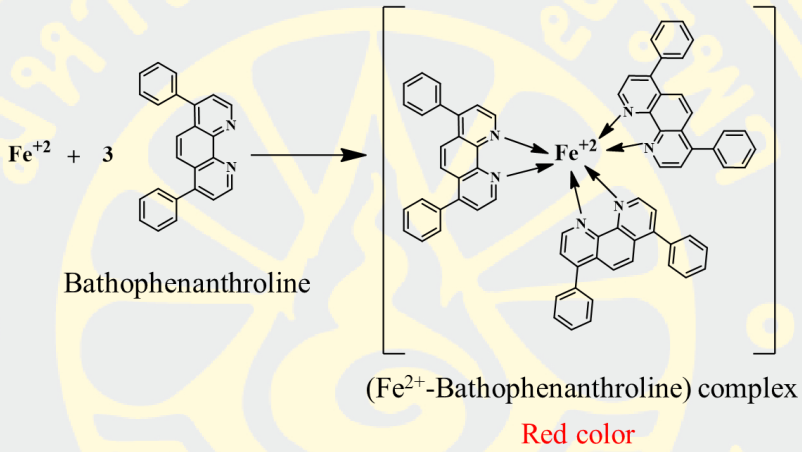

Figures 4-3 Reaction between Fe^{2+} and Bathophenanthroline reaction.

This research investigated optimal conditions that could be further used for the simultaneous detection of water hardness, chloride, and iron in a single step, aiming for user-friendly and accurate analysis. The studied conditions are outlined below.

4.2 Optimization of the proposed assay

4.2.1 Water hardness assay

4.2.1.1 Type of buffer

Types of buffers used in paper-based assay were investigated. For classical titration of Ca^{2+} and Mg^{2+} with EDTA, an ammonia buffer at pH 10 was used. In this work, the ammonium buffer was test by dissolving EBT in this buffer deposited on the devices. However, volatile ammonia is unsuitable which results in a change in the pH value resulting in the change of EBT color, as shown in Figure 4-4A. A buffer for a μPAD should have a pKa close to the desired pH and remain stable as a solid at room

temperature. Hence, the CAPS buffer was employed to prepare a buffer solution at pH 10 as its pKa is 10.6. Observations revealed a color change to magenta on the paper device and the formation of a white precipitate at the hydrophobic barrier that might influence water hardness detection (Figure 4-4B) making it not suitable for use. Finally, the glycine buffer solution (pKa of 9.78) pH 10 was tested and found to be suitable for µPAD use. As shown in Figure 4-4C, stable blue color on the paper device was observed and can be used for water hardness detection. Consequently, the glycine buffer solution was selected for further experiments.

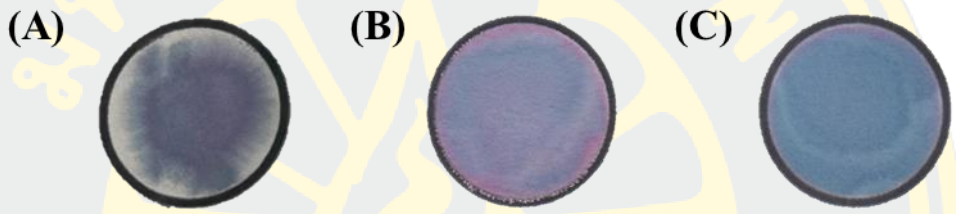

Figures 4-4 Selecting the type of buffer for water hardness analysis. (A) NH_3/NH_4Cl buffer solution (1.1 mM, pH 10) (B) CAPS buffer solution (1M, pH 10), (C) Glycine buffer solution (0.4 M, pH 10).

4.2.1.2 Reagent deposition sequence and lamination

The investigation into reagent deposition sequence on the measuring device was studied including: two-step and one-step deposition methods. Two step deposition method was carried out by depositing the buffer solution followed by the EBT solution. For each reagent deposition, the device was allowed to dry. In one-step deposition, the EBT solution prepared in glycine buffer solution was added directly onto the test zone and the device was allowed to dry. Figures 4-5A and B shows devices prepared by the two-step deposition method before and after water hardness testing. Figure 4-5C and D shows devices prepared by the two-step deposition method before and after water hardness testing. Both types of reagents deposition gave similar results. Therefore, one-step reagent deposition was selected for further study as it provided more convenient reagent deposition.

The impact of clear plastic coating on the developed devices was evaluated. In Figure 4-5E, the paper device without clear plastic coating showed nonuniform color

band on the device after testing. Therefore, clear plastic coating was applied, which effectively controlled solution flow direction. (Figure 4-5F)

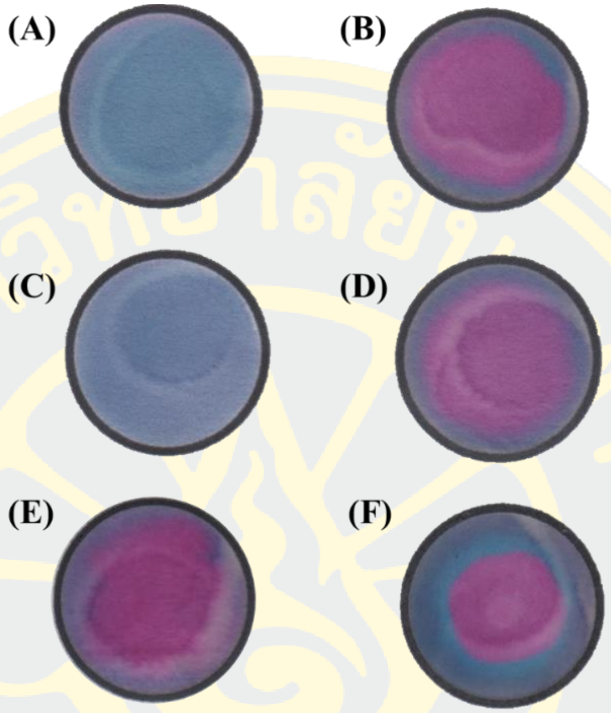

Figures 4-5 (A) Two-step glycine buffer solution (0.40 M, pH 10) before test with 0.8 mM of Ca^{2+} and Mg^{2+} (B) Two-step glycine buffer solution after test. (C) One-step glycine buffer solution (0.40 M, pH 10) before test with 0.8 mM of Ca^{2+} and Mg^{2+} (D) One-step glycine buffer solution after test. (E) One-step for without lamination plastic. (F) One-step for lamination plastic.

4.2.1.3 Reagent deposition method for simultaneous analysis

Reagent deposition on a paper-based device for simultaneous analysis was evaluated. The first method involved dropping a 0.5 mM EBT in glycine buffer solution at pH 10 onto the device and rolling it over the test area. Uneven spreading of the dropped solution was observed in the test area due to the coffee ring effect. (Maria Smolinska, 2015) (Figure 4-6A). Subsequently, the second method was tried by immersing the device in the EBT solution, which proved to be more effective. This method provided uniform distribution across the test area, resulting in smooth and consistent coloration (Figure 4-6B). However, the immersing of the entire device into the EBT solution might not be suitable depositing reagents on a device prepared for

simultaneous analysis. Therefore, a tapping method was employed for reagent deposition. In this method, a drop of 30 µL EBT solution was placed on a clean surface and the water hardness test zone was tapped directly onto the reagent drop to absorb the reagent into the test zone with uniform distribution (Figure 4-6C).

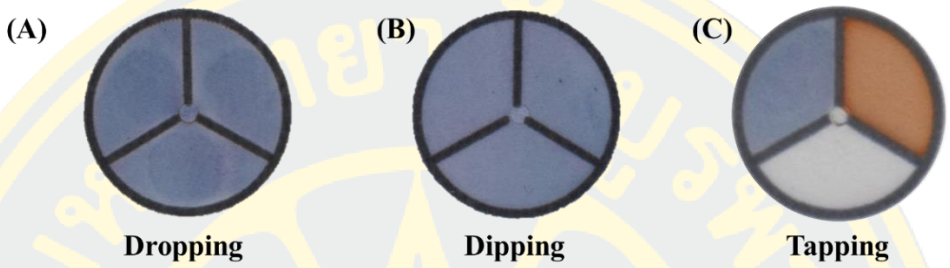

Figures 4-6 Study the effect of reagent deposition on a paper-based device. (A) Dropping 100 µL of 0.5 mM EBT + glycine buffer solution (pH 10, 0.48 mM). (B) Dipping device to 0.5 mM EBT + glycine buffer solution (pH 10, 0.48 mM). (C) Tapping device for simultaneous analysis.

4.2.1.4 Concentration of buffer

The concentration of the glycine buffer solution at pH 10 was initially optimized, as the reaction between EBT and Ca^{2+}/Mg^{2+} occurs and induces a color change at pH 10. Glycine concentrations of 0.4 M and 0.48 M were investigated. It was observed that the 0.48 M glycine buffer at pH 10 produced a more distinct color change on the test zone when a 0.5 mM mixture standard of Ca^{2+}/Mg^{2+} was added compared to the 0.4 M glycine buffer at pH 10 (Figure 4-7). Higher buffer concentrations yield better pH control. Therefore, a glycine buffer concentration of 0.48 M at pH 10 was selected as the optimal concentration and used for further experiments.

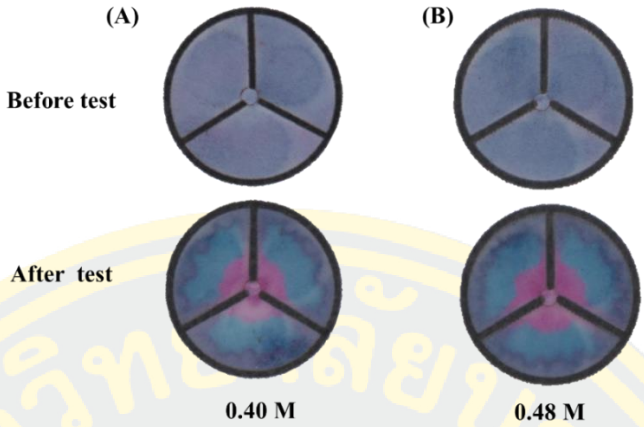

Figures 4-7 Study the concentration of 0.5 mM EBT + Glycine buffer solution pH 10 (A) concentration 0.40 M (B) concentration 0.48 M (tested with mixed solution of 0.5 mM Ca^{2+}+Mg^{2+}).

4.2.1.5 Glycine buffer range

The effect of glycine buffer in the pH range of 8-12 on the analysis was evaluated (Figure 4-8). At pH range of 8-9, the red-purple circles in the radial distance were unclear when tested with 2.5 mM Ca^{2+} and Mg^{2+} solutions. (Maurya, 2023) On the other hand, at the pH range of 10-12, the magenta circles in the radial distance were clearly visible, facilitating easy observation of radial distance. Therefore, in this experiment, a pH 10 buffer solution was chosen as the most suitable and sufficient range for testing water hardness.

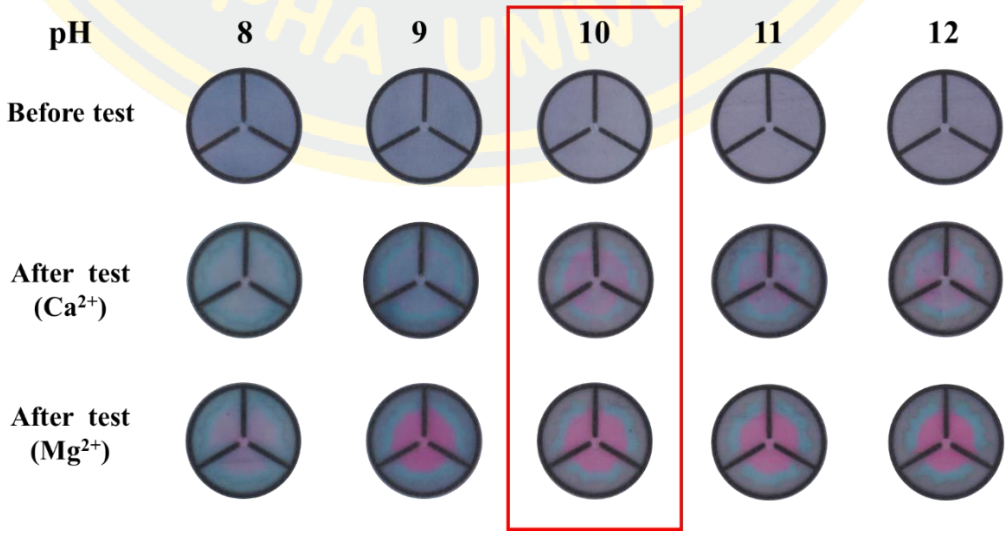

Figures 4-8 Study the effect of the pH of the glycine buffer solution.

4.2.1.6 EBT concentration

Optimization of EBT concentration was carried out next to enhance test sensitivity. Various concentrations (0.1, 0.5, 1, and 2 mM) were tested, resulting in different levels of blue intensity, with higher concentrations yielding darker blue color intensities (Figure 4-9). Subsequently, devices were tested with standard Ca^{2+} and Mg^{2+} solution mixture (2.5 mM), resulting in the formation of Ca/Mg-EBT magenta complex in all devices. The radial distance of these complexes decreased with increasing EBT concentration due to variations in EBT density on the paper test zone. Lower EBT density required a larger area for complete reaction with Ca^{2+}/Mg^{2+}, and at an EBT concentration of 0.1 mM, the radial distance of the formed magenta product was unclear and difficult to observe. Therefore, a concentration of 0.5 mM EBT was selected for the next experiment due to its better signal radial distance and sufficient magenta color intensity for observation.

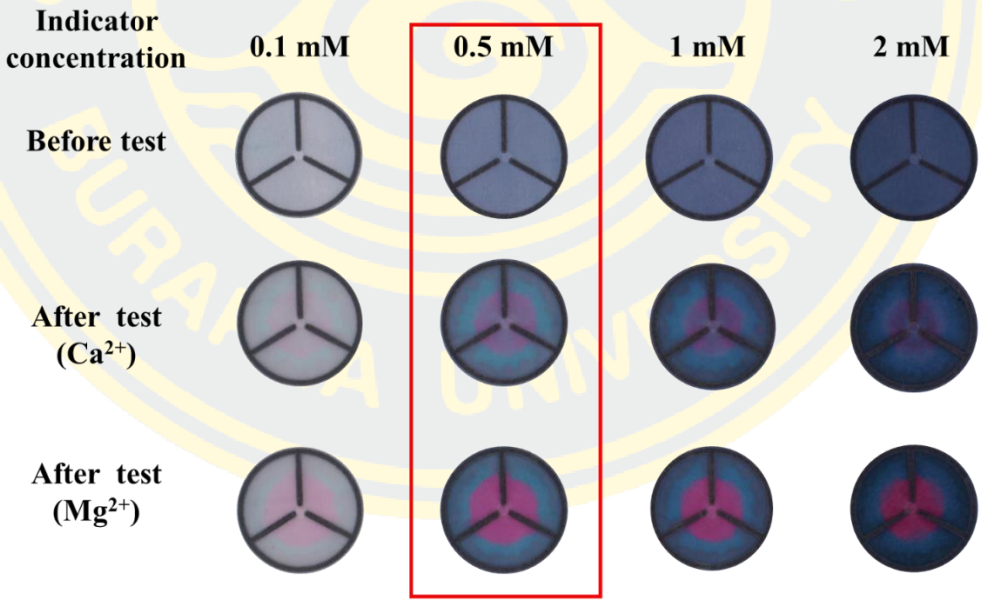

Figures 4-9 The study of optimal concentration of Eriochrome black in the concentrations of 0.1, 0.5, 1, and 2 mM.

4.2.2 Chloride assay

4.2.2.1 Reagent deposition method

Deposition method of $AgNO_3$ and $Cr_2O_4^{2-}$ reagent onto the paper-based devices was investigated in similar manner to that of EBT deposition for water hardness including dropping, dipping and tapping methods. The dropping method was carried out by dropping 100 µL 50 mM $AgNO_3$ and allowed to dry followed by dipping the device into 50 mM $Cr_2O_4^{2-}$ solution. Similar result to EBT dropping deposition method was observed as the coffee ring effect cause an ununiform color precipitated all over the test zones. Therefore, dipping and tapping of the device in the $AgNO_3$ and $Cr_2O_4^{2-}$ solution was carried out and the uniform precipitate of Ag_2CrO_4 was obtained in both cases (Figure 10). Therefore, dipping and tapping methods was employed from reagent deposition in single analyte, multi-analyte analysis, respectively.

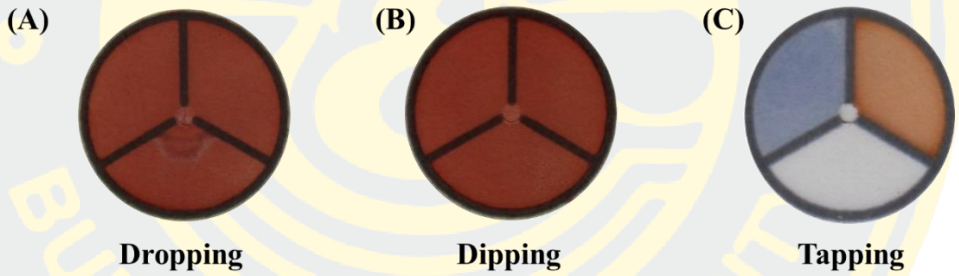

Figures 4-10 Study the effect of reagent deposition on a paper-based device. (A) Dropping $AgNO_3$ solution let dry and then dip the device into $Cr_2O_4^{2-}$ solution (pH 7.2, 50 mM). (B) Dipping the device in 100 µL of $AgNO_3$ solution and letting it dry, then dipping into $Cr2O_4^{2-}$ solution (pH 7.2, 50 mM). (C) Tapping device for simultaneous analysis.

4.2.3 Iron assay

4.2.3.1 Concentration of reagent

The concentration of Bphen in the range of 2.5-20 mM was optimized for iron assay. After tested with 20 mg/L Fe^{2+}, the red color of Fe(II)-Bphen complex appeared where the higher the Bphen concentration used, the narrower the red color radial distance observed (Figure 4-11) as a results of the variation of reagent availability per test zone unit area for Fe^{2+} reaction. In this test, Bphen was selected at a 1 mM and used

for further experiments because it provided an observable color with high radial distance.

Figures 4-11 Study the optimal concentration of Bphen on the paper-based device for Fe^{2+} analysis.

4.3 Analysis of single analyte using the developed paper-based sensors

4.3.1 Water hardness analysis

The level of water hardness was assessed by analyzing a solution containing calcium ions (Ca^{2+}). The concentration of calcium ions was quantified and expressed as the equivalent concentration of calcium carbonate ($CaCO_3$). The apparent radial distance of the magenta color increased as the water hardness increased.

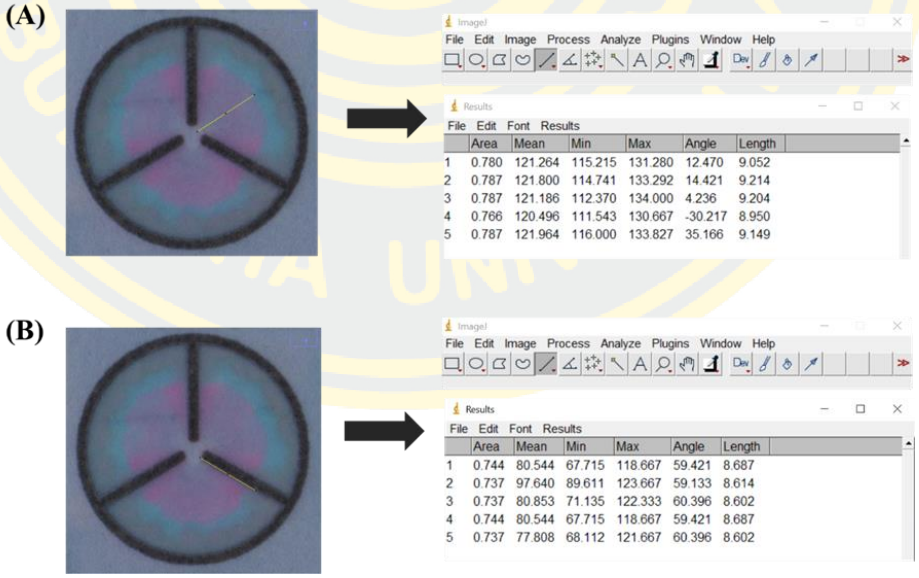

Figures 4-12 Measuring radial distance signal on the developed paper-based devices at (A) The central area (B) Edge area.

A calibration curve plotting of radial distance of magenta color measured at the edge and the central (Figure 4-12A-B) of the band against $CaCO_3$ concentration

giving the linear range of 25-1501 mg/L. This range covered the water hardness at every level including soft (0 - 75 mg/L), moderately hard (75–150 mg/L), hard (150–300 mg/L) and very hard (>300 mg/L). (Al-Khashman, Alnawafleh, Jrai, & Al-Muhtaseb, 2017) Moreover, similar sensitivities were obtained for both measurement at the edge and central area of the magenta signal indicating the negligible errors from measuring in different positions of the color radius. A little lower of the sensitivity obtained from the edge area measurement was a result of flow delay by the capillary wall involving wax hydrophobic barrier. Limit of detection defined as the lowest concentration of $CaCO_3$ concentration that can be reliably detected using the formula of 3.3SD/slope where the SD and slope is the standard deviation of the blank and slope of the calibration, respectively, the LOD using a paper-based device developed for water hardness analysis was 1 mg/L and 1.14 mg/L for the central and edge area respectively, This LOD was lower than that reported for water hardness analysis which was 0.5 mM. (Karita & Kaneta, 2016) The repeatability obtained from the analysis of water hardness with the concentration in the linear ranges for the radius measurement at the edge and center position reported as relative standard deviation (%RSD) gave high repeatability in the range of 0.54-5.77% and 0.79-4.87%, respectively. These values fall within the acceptable range according to AOAC standards. (AOAC International, 2016)

To verify the accuracy of the water hardness assay using the developed paper-based sensor, water samples collected from various sources including tap water, pond water, boiler and cooling water were analyzed using the developed method and the traditional EDTA titration method. The results showed that the water hardness expressed as $CaCO_3$ obtained from the developed method and the titration method are not statistically different at 95% confidence level (two tailed P = 0.07) as shown in Table 4. These results indicated the accuracy of the developed assay to be comparable with the traditional method for water hardness determination.

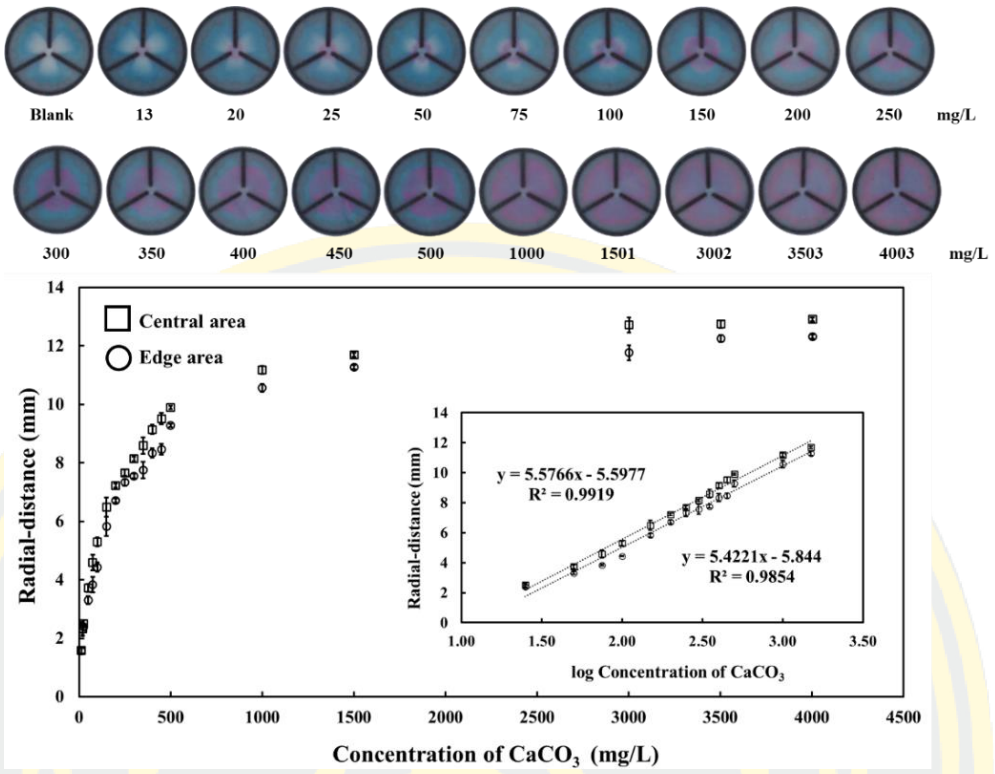

Figures 4-13 A plot of radial distance of the magenta color as a function of $CaCO_3$ in the range of 13-1001 mg/L. (n = 6). (Inset) Linear range of calibration from 25-1501 mg/L (R^2 = 0.9919 for central area measurement and R^2 = 0.9854 for edge area measurement).

Table 4. Water hardness content obtained from the developed paper-based assay and the traditional titration methods.

Samples	Concentration of Water Hardness (mg/L)	
	Proposed sensor (n=3)	Titrate (n=3)
	mg/L ± SD	mg/L ± SD
Tap water 1	72.59 ± 1.56	70.39 ± 0.58
Tap water 2	67.50 ± 2.63	65.06 ± 0.00
Tap water 3	77.71 ± 2.70	78.74 ± 1.16
Tap water 4	86.67 ± 1.64	84.41 ± 0.58
Tap water 5	24.42 ± 0.10	19.35 ± 0.58
Tap water 6	82.55 ± 0.70	78.40 ± 0.76
Pond water 1	288.60 ± 12.67	246.88 ± 1.16
Pond water 2	129.78 ±4.01	109.09 ± 1.00
Boiler system	ND	ND
Cooling system	501.94 ± 10.94	493.09 ± 10.58

N.D.= Not detected

4.3.2 Chloride assay

Chloride was detected based on the Mohr precipitation titration but in a reverse manner as the chloride ions replaced with the chromate ions on the deposited silver chromate precipitate creating the white precipitate of silver chloride. (Rahbar et al., 2019) Under optimal condition, different chloride concentrations were measured and the results showed in Figure 4-14. As the Cl^- concentration increased the radial diameter of the white precipitates increased. The plot of radial diameter of the white precipitate as a function of chloride concentration was generated yielding the linear range of 0.25-100 mM where higher sensitivity was obtained from the measurement at the central area of the white precipitate as a result of higher flow at the central than that of the edge. The limit of detection was 0.25 mM for the central and edge measurements visible to the naked eye. High repeatability was also obtained which are in the RSD range of 0.82-8.63%. The water samples were then analyzed using the developed paper-based assay and the results validated with those obtained from the traditional Mohr's titration method to prove the accuracy. (Di Leo & Sardanelli, 2020) For all 10 water samples, the chloride content obtained from the two methods are not significantly differences at 95% confidence interval (two tailed $P > 0.06$) indicating the high accuracy of the developed methods confirming that the proposed method is a viable alternative for analyzing chloride in water. (Table 5).

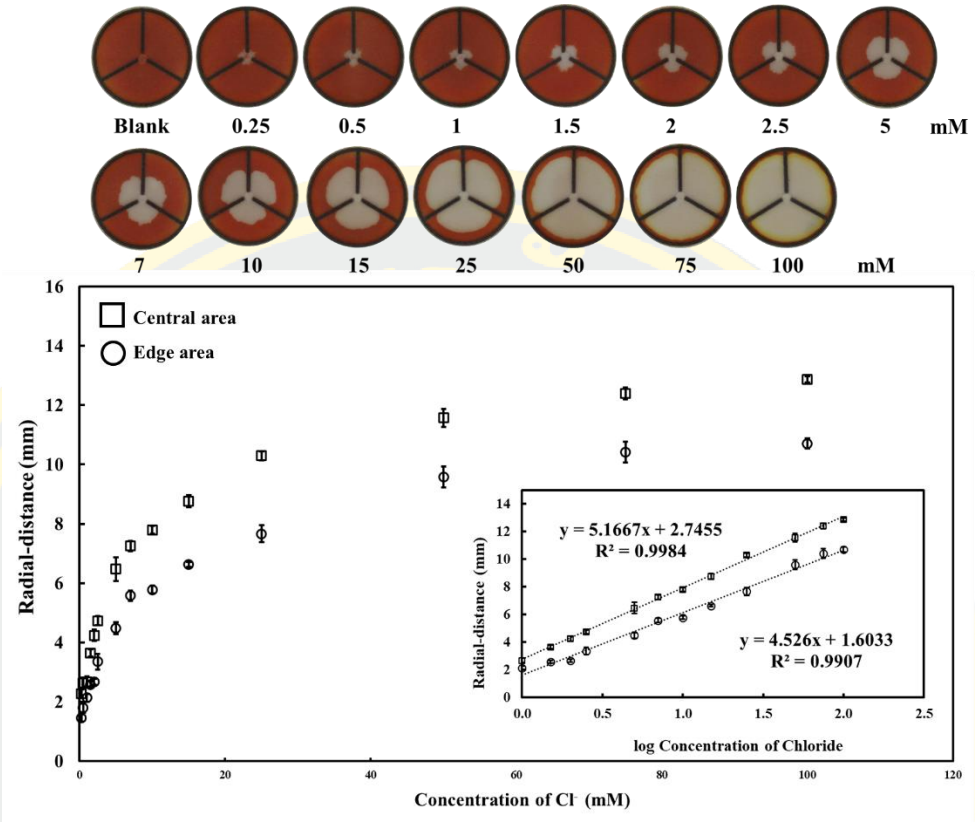

Figures 4-14 Plot of radial distance as a function of chloride concentration (n = 6). (Inset: a linear range of calibration from 1-100 mM (R^2 = 0.9984 of central area and R^2 = 0.9907 of edge area)

Table 5. Chloride content in water samples obtained from the developed paper-based devices and Mohr precipitation titration.

Samples	Concentration of Chloride (mM)	
	Proposed sensor (n=3)	Titrate (n=3)
	mM ± SD	mM ± SD
Tap water 1	1.31 ± 0.08	1.27 ± 0.01
Tap water 2	5.14 ± 0.26	5.17 ± 0.10
Tap water 3	10.53 ± 0.50	10.89 ± 0.10
Tap water 4	2.48 ± 0.16	2.46 ± 0.01
Tap water 5	1.07 ± 0.04	0.82 ± 0.06
Tap water 6	0.83 ± 0.05	0.58 ± 0.10
Pond water 1	18.73 ± 0.21	18.31 ± 0.12
Pond water 2	5.99 ± 0.30	5.10 ± 0.16
Boiler system	7.67 ± 0.27	7.42 ± 0.10
Cooling system	9.32 ± 0.09	8.61 ± 0.12

4.3.3 Iron assay

Iron was detected using bathophenanthroline (Bphen) that reacts with Fe^{2+} under acidic conditions (pH 4.5) to form the red complex product. (Véronique Rouchon a, 2013) Bphen was chosen as a chromogenic reagent for Fe^{2+} and was selected over 1,10-phenanthroline due to its higher sensitivity and reduced interference in detecting Fe^{2+}. (Cate et al., 2015; Charleton, Smith, & Goltz, 2009) Unlike traditional phenanthroline, Bphen is less prone to the coffee ring effect due to its lower solubility. (Aryal et al., 2023) The higher the Fe^{2+} investigated, the more the radial distance of red color obtained (Figure 4-15). A plot the radial distance as a function of Fe^{2+} concentration was generated giving a linear range for Fe^{2+} of 0.5-300 mg/L. The limit of detection was 0.5 mg/L for the central and edge measurements visible to the naked eye. The high repeatability obtained from the replicate measurement of the Fe^{2+} with the concentration in the linear range was found in the range of 0.27-7.57% for both types of measurement.

To verify the accuracy, water samples were analyzed using the developed paper-based sensor and the results compared to those obtained from traditional spectrophotometry assay (Table 6). The Fe^{2+} contents in all samples obtained both assays were not significant different at 95% confidence interval (two tailed $P > 0.05$). Moreover, the recovery for all samples was in the range of 85−106% indicating that the acceptable accuracy of the developed device for Fe^{2+} analysis in the investigated water samples was obtained.

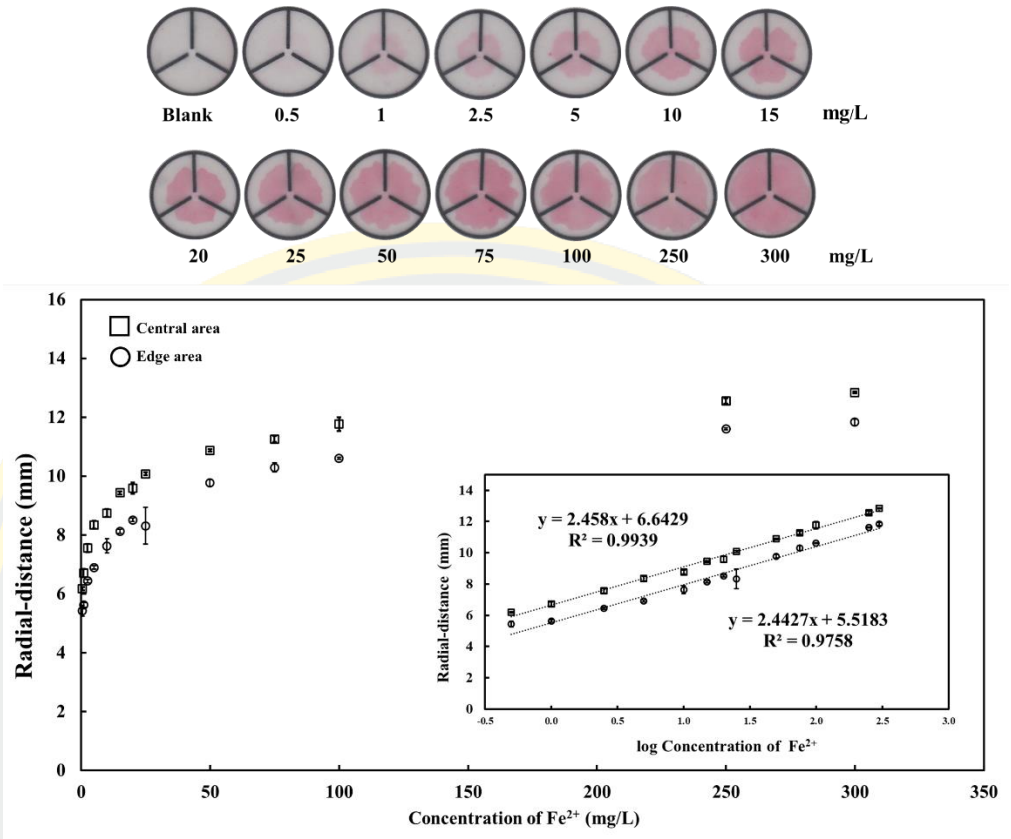

Figures 4-15 Plot of radial distance as a function of Fe^{2+} concentration (n = 3) with a linear range of 0.5-300 mg/L (R^2 = 0.9939 of central area and R^2 = 0.9758 of edge area).

Table 6. Iron analysis in water samples using the developed paper-based assay and the spectrophotometric assay.

Samples	Spiked [Fe] mg/L	Proposed sensor (n=3)			Spectrophotometry (n=3)		
		Found (mg/L)	%Recovery	%RSD	Found (mg/L)	%Recovery	%RSD
Groundwater	0	N.D.			N.D.		
	3	3.56 ± 0.35	85	13.8	2.69 ± 0.04	90	1.35
	15	15.88 ± 0.99	99	6.6	15.07 ± 0.05	100	0.28
	50	54.02 ± 4.03	106	7.6	50.27 ± 0.14	101	0.26
Pond water 1	0	N.D.			N.D.		
	3	3.59 ± 0.22	86	8.4	2.82 ± 0.09	94	3.29
	15	16.86 ± 1.35	106	8.5	14.88 ± 0.21	99	1.38
	50	52.96 ± 2.21	104	4.3	48.72 ± 0.23	97	0.47
Pond water 2	0	N.D.			N.D.		
	3	3.72 ± 0.38	91	14.14	2.94 ± 0.01	98	0.44
	15	14.92 ± 1.39	93	9.96	15.54 ± 0.11	104	0.69
	50	47.52 ± 4.98	93	10.7	48.68 ± 0.79	97	1.62
Boiler system	0	N.D.			N.D.		
	3	3.55 ± 0.21	85	8.15	2.92 ± 0.03	97	0.9
	15	15.22 ± 1.46	95	10.25	15.05 ± 1.13	100	7.5
	50	46.67 ± 5.05	91	11.07	47.24 ± 0.51	94	1.08
Cooling system	0	N.D.			N.D.		
	3	3.29 ± 0.28	86	10.74	2.91 ± 0.03	97	0.99
	15	16.52 ± 1.19	103	7.68	15.18 ± 0.07	101	0.46
	50	48.19 ± 4.77	94	10.11	49.13 ± 0.24	98	0.49

The analytical results for these three tests are summarized in Table 7. The tests measure two types of radial distances: at the center and edge of the test area. It was observed that measurements at the center test area provided better sensitivity and R^2 compared to those at the edge area. These results demonstrate the effectiveness of the developed paper sensor, enabling the detection of water samples containing hardness, chloride, and iron.

Table 7. Analytical figures of merit for water hardness, chloride, and iron detection using developed paper-based devices.

Target ion	Type	Linear range	Linear equation	LOD	%RSD
Ca^{2+} as equivalent to $CaCO_3$ (n=6)	Central area	25-1501 mg/L	y = 5.5766x - 5.5977 R^2 = 0.9919	1.00 mg/L	0.54-5.77%
	Edge area	25-1501 mg/L	y = 5.4221x - 5.844 R^2 = 0.9854	1.14 mg/L	0.79-4.87%
Cl^- (n=6)	Central area	1-100 mM	y = 5.1667x + 2.7455 R^2 = 0.9984	0.25 mM	0.82-6.33%
	Edge area	1-100 mM	y = 4.526x + 1.6033 R^2 = 0.9907	0.25 mM	1.32-8.03%
Fe^{2+} (n=3)	Central area	0.5-300 mg/L	y = 2.458x + 6.6429 R^2 = 0.9939	0.5 mg/L	0.27-2.13%
	Edge area	0.5-300 mg/L	y = 2.4427x + 5.5183 R^2 = 0.9758	0.5 mg/L	0.31-7.57%

4.4 Interference Studies

The potential interferences typically present in water were investigated for each assay detection. For every test, a standard solution of each analyte (1 mM Ca^{2+}, 1 mg/L Fe^{2+}, 1 mM Cl^{-}) was mixed with varying concentrations of each interference and then analyzed using the developed paper-based sensor. Interfering ions were considered to affect the analysis of each analyte if the measured radial distance differed significantly from that obtained with the analysis of 1 mM of each analyte alone, as determined by a pooled variance t-test at a 95% confidence level. For water hardness, cations including Na^{+}, Li^{+}, K^{+}, Zn^{2+}, Cu^{2+}, Ni^{2+}, Hg^{2+}, and Al^{3+} were tested. (Shibata et al., 2019) As shown in Figure 4-16A, the assay demonstrated high tolerance to most ions, with tolerance levels exceeding 1 mM for interfering ions. While, Zn^{2+} at 1 mM was observed to interfere with the assay, this is unlikely to pose a problem given that water samples typically contain much lower concentrations of Zn^{2+} (6-12 ng/mL). (Abkenar, Dahaghin, Sadeghi, Hosseini, & Salavati-Niasari, 2011)

For chloride, interferences including Fe^{2+}, Fe^{3+}, Zn^{2+}, Cu^{2+}, F^{-}, PO_4^{3-}, SO_4^{2-}, and HCO_3^{-} were investigated. (Aryal et al., 2023) The developed assay has high tolerance to all studied anions but demonstrates low tolerance to heavy metal ions at concentrations higher than 0.05 mM (Figure 4-16B). However, these cations are regulated by the World Health Organization (WHO) to be present in water samples in the range of 0.1 μM–0.031 mM which are much lower than chloride ions. Therefore, we anticipated that the developed assay would not be affected by these heavy metal ions.

Finally, interfering ions for Fe^{2+} assay were investigated including Zn^{2+}, Cu^{2+}, Co^{2+}, Mg^{2+}, Ni^{2+}, PO_4^{3-}, SO_4^{2-}, and HCO_3^{-}. (Aryal et al., 2023) The results show that the assay has high tolerance to the interfering ions where more than 1:10 concentration ratio of the Fe^{2+} and the investigated ions was still found to not interfere (Figure 4-16C). Moreover, these ions are found to be much lower concentration in real water samples. (Al-Khashman et al., 2017; Olowu et al., 2010; R. Rajendran1, 2015; Sarma, 2018; Thatai, Verma, Khurana, Goel, & Kumar, 2019).

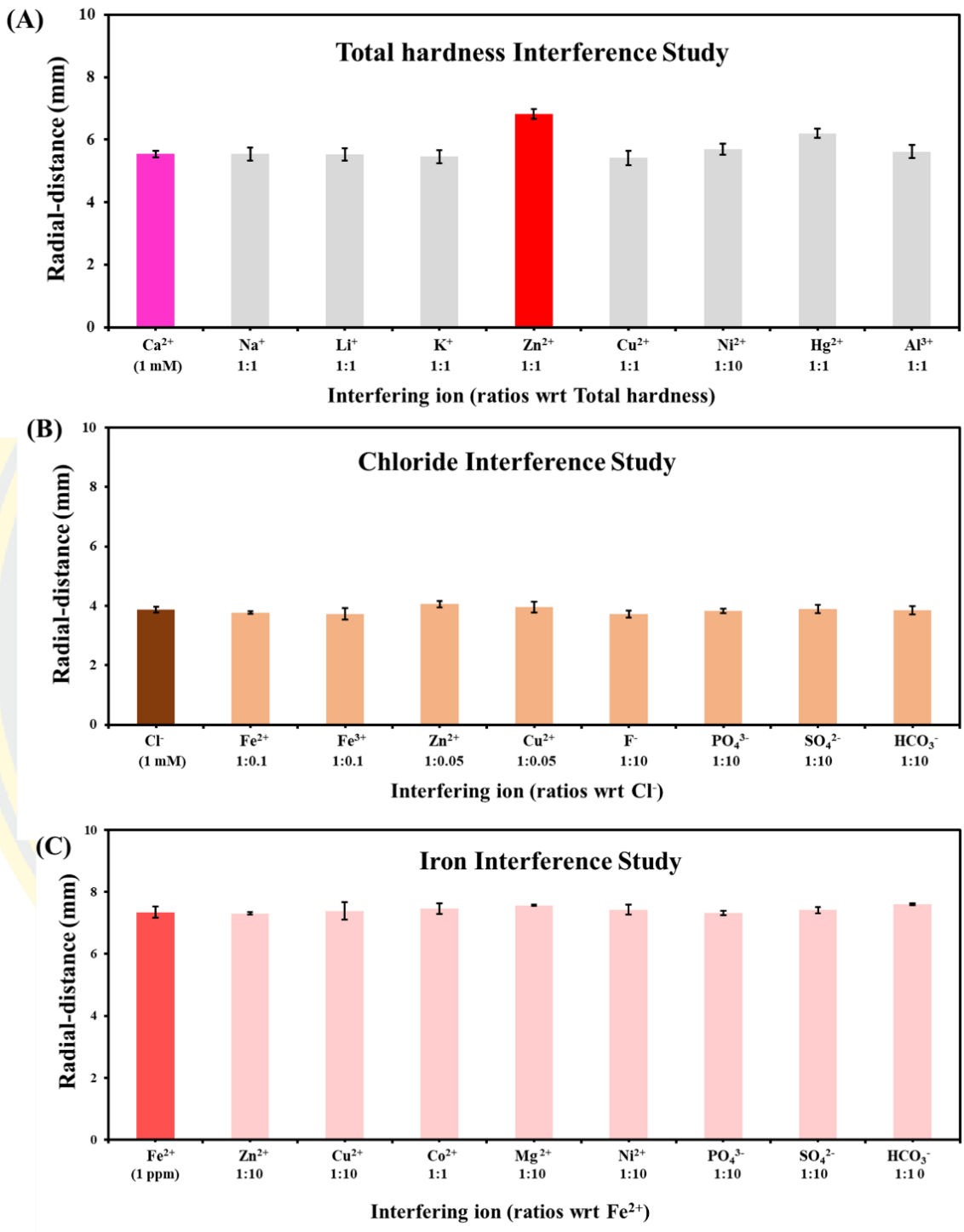

Figures 4-16 Interference study for all three assays. (A) 1:1 and 1:10 mM ratios. (B) 1:0.05, 1:0.1 and 1:10 mM ratios. (C) 1:1 and 1:10 mg/L ratios. Red bars indicate signal changes.

4.5 Storage Stability Study

The stability of the prepared devices was evaluated under various storage conditions including room temperature (25-38°C, RT Dark) and in the fridge at 6-10°C for 2 months. All devices were prepared at the same time, stored in Mylar and Ziplock bags and tested every week using 1.5 mM of mixture of equal amount of Ca^{2+} and Mg^{2+}, 7 mM of Cl^- and 1 mg/L Fe^{2+} for water hardness, chloride and iron analysis respectively. at these temperatures are shown in Figure 6. The results were compared to those obtained from the analysis using the freshy prepared devices and expressed as %radial distance. For all three assays, the devices were found to be stable for more than 2 months as the %radial distance did not significant different to 100% for all two storage conditions. The variation was found to be in the range of random error reported as the repeatability described above. It is advisable to store the device Mylar bag to prevent deterioration and minimize exposure to light and moisture. (Menger, Beck, Borch, & Henry, 2022)

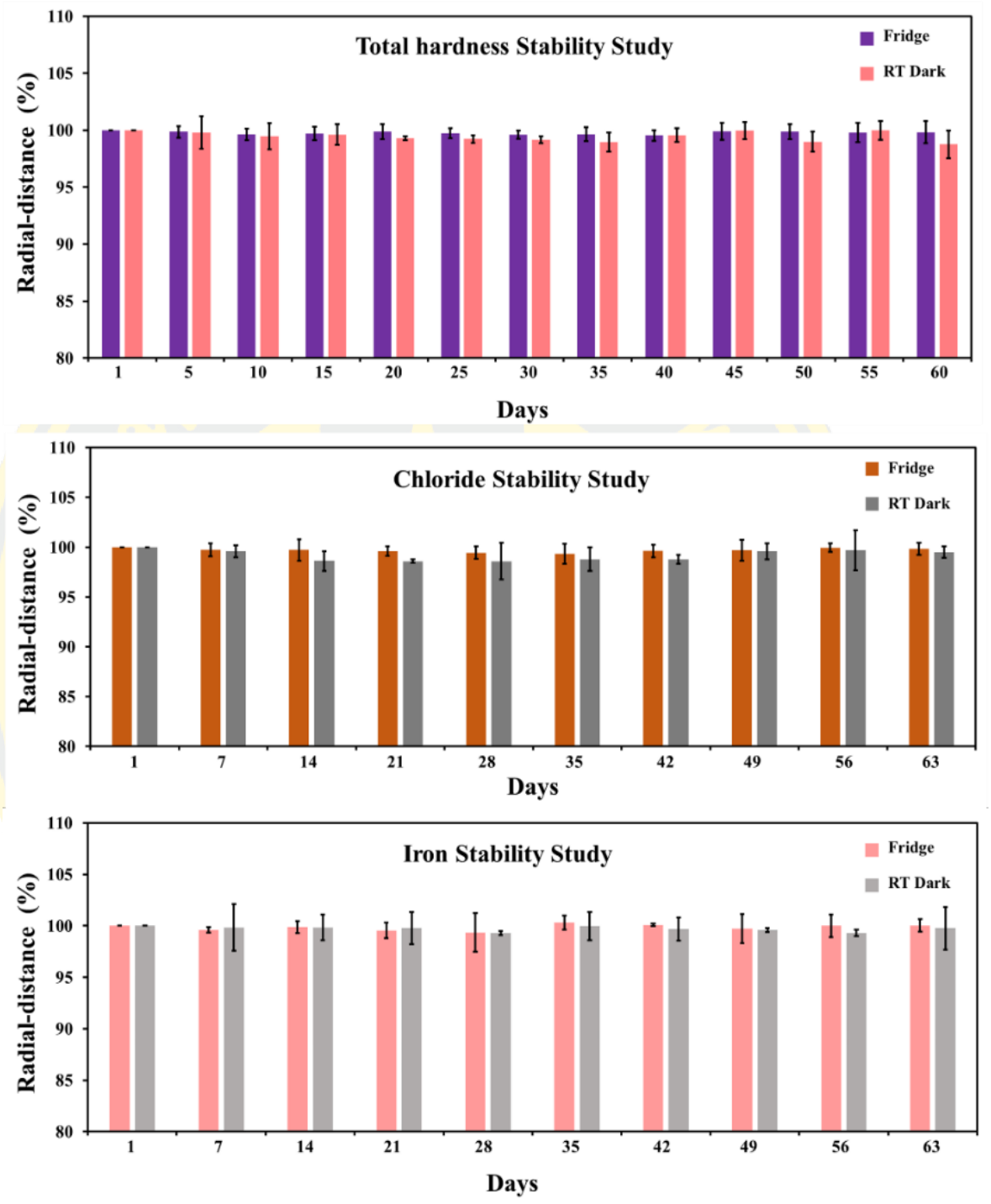

Figures 4-17 Storage stability of paper-based devices in all three tests (n=3) when kept in Fridge at 6-10°C and Room Temperature in the Dark (RT Dark) at 25-38°C.

4.6 Simultaneous analysis of water hardness, chloride and iron

The devices were next used to simultaneously analyze water hardness, chloride, and iron in real water samples. The paper-based device was prepared using optimal conditions with some modifications. The chromate buffer concentration was changed from 50 mM to 100 mM for chloride detection zone to increase the buffer capacity since the pH of water samples were needed to be adjusted to 4.5 for Fe^{2+} detection at the other test zones. The increasing in chromate buffer concentration did not impact on the analysis of chloride (Figure 4-18).

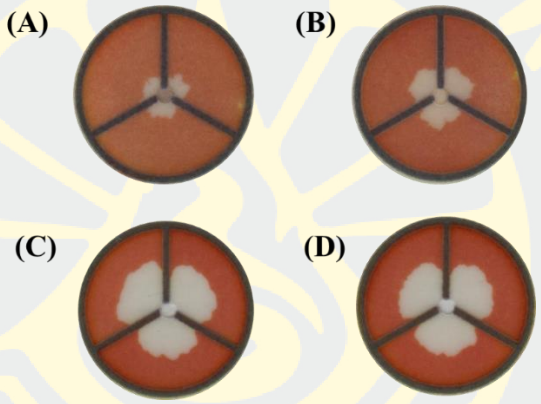

Figures 4-18 (A) 12.5 mM $AgNO_3$, Chromate Buffer (pH 7.2, 50 mM) with 1 mM Cl^- using deionized water. (B) 12.5 mM $AgNO_3$, Chromate Buffer (pH 7.2, 50 mM) with 1 mM Cl^- using acid deionized water. (C) 12.5 mM $AgNO_3$, Chromate Buffer (pH 7.2, 100 mM) with 7 mM Cl^- using deionized water. (D) 12.5 mM $AgNO_3$, Chromate Buffer (pH 7.2, 100 mM) with 1 mM Cl^- using acid deionized water

Moreover, the pH adjustment to 4.5 did not impact the simultaneous analysis of the three target analytes using the radial distance-based measurement paper device. Although the color intensity might be affected when the pH changed especially for water hardness detection, the radial diameter obtained from the analysis of water samples after pH adjustment were similar to that of before pH adjustment (Figure 4-19C and D and Table 8). This result indicated that the measurement using radial distance-based readout provided more robustness in analytical performance than the color intensity-based readout. For all original water samples, there are some levels of water hardness and chloride were observed where the tap and cooling water were found to have high chloride and water hardness than that of the ground and pond water. However, the Fe^{2+} was found as not detected for all samples indicated that low level of this analyte in the investigated samples. To test the accuracy of the developed assay as a simultaneous analysis, the Fe^{2+} at the concentration of 1 mg/L was spiked to all samples. The results demonstrated a recovery range of 105−110% for all samples, indicating the acceptable accuracy of the developed device for Fe^{2+} analysis in the tested water samples. (Table 9). For chloride and hardness, the concentrations of the analytes in the evaluated samples obtained from the simultaneous analysis using the developed paper-based devices were not significant difference from those obtained from traditional assays at 95 % confidence level (the two tailed $P = 0.27$ for water hardness and $P = 0.23$ for chloride). These results indicated that the develop paper-based method provided accurate analysis for simultaneous measurement of chloride, hardness and iron and can be used as an alternative tools for fast and on-site assessment of water quality.

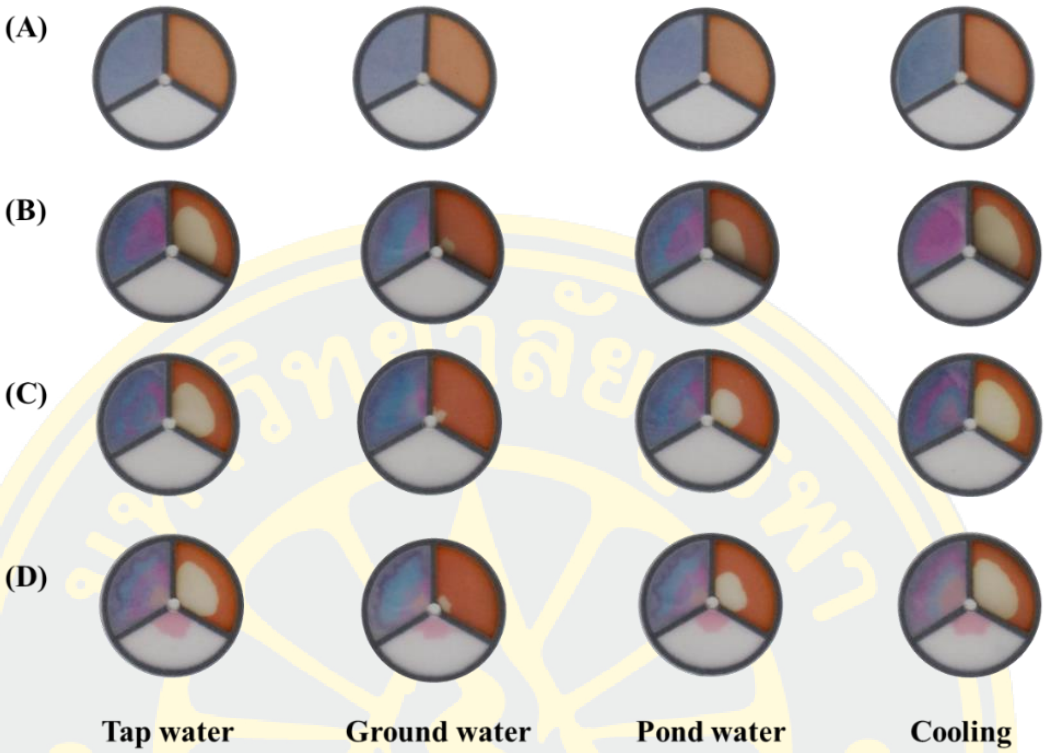

Figures 4-19 Simultaneous analysis of water hardness, chloride, and iron in real water samples. (A) Paper-based device developed before testing with the samples. (B) The device after testing with water samples without pH adjustment. (C) The device after testing with water samples with the pH adjusted to 4.5. (D) The device after testing with water samples with the pH adjusted to 4.5 and spiked with 1 mg/L Fe^{2+}standard solution.

Table 8. Radial distance of the water samples tested by the developed paper-based devices. (n=3)

Samples	Tap water	Ground water	Pond water	Cooling
1. Water sample without pH adjustment				
Radial distance total hardness (mm)	8.22 ± 0.11	5.42 ± 0.26	7.07 ± 0.03	10.05 ± 0.09
Radial distance chloride (mm)	8.41 ± 0.26	2.71 ± 0.07	6.89 ± 0.10	8.99 ± 0.05
Radial distance iron (mm)	-	-	-	-
2. Water sample was adjusted to pH 4.5				
Radial distance total hardness (mm)	8.17 ± 0.14	5.42 ± 0.01	7.02 ± 0.14	10.11 ± 0.15
Radial distance chloride (mm)	8.36 ± 0.15	2.25 ± 0.06	6.49 ± 0.35	8.85 ± 0.05
Radial distance iron (mm)	-	-	-	-
3. Water sample was adjusted to pH 4.5 with the addition 1 mg/L Fe^{2+} standard solution				
Radial distance total hardness (mm)	8.12 ± 0.03	5.38 ± 0.12	7.19 ± 0.18	10.17 ± 0.10
Radial distance chloride (mm)	8.47 ± 0.31	2.66 ± 0.22	6.49 ± 0.12	8.86 ± 0.03
Radial distance iron (mm)	6.74 ± 0.07	6.67 ± 0.07	6.70 ± 0.11	6.62 ± 0.08

Table 9. Water hardness, chloride, and iron contents in water samples obtained from simultaneous analysis using developed paper-based assays and the traditional assay (n = 3).

Samples	Concentration of water hardness (mg/L± SD)		Concentration of chloride (mM± SD)		Concentration of iron (mg/L± SD)		
	Proposed sensor	Titrate	Proposed sensor	Titrate	Added	Proposed sensor	Recovery
Tap water	250.55 ± 13.94	180.82 ± 0.58	12.61 ± 0.94	11.02 ± 0.06	0	ND	
					1	1.09 ± 0.07	109%
Ground water	96.38 ± 4.19	85.74 ± 0.58	0.89 ± 0.11	0.65 ± 0.06	0	ND	
					1	105 ± 0.02	105%
Pond water	166.46 ± 9.72	136.12 ± 1.00	5.25 ± 0.27	5.36 ± 0.06	0	ND	
					1	1.10 ± 0.06	110%
Cooling	690.35 ± 25.36	248.55 ± 2.89	15.07 ± 0.50	14.60 ± 0.11	0	ND	
					1	1.06 ± 0.06	106%

N.D.= Not detected

CHAPTER 5
CONCLUSIONS AND FUTURE PERSPECTIVES

5.1 Conclusions

In this work, the paper-based sensor for simultaneous detection of water hardness, chloride, and iron in real water samples has been successfully developed. Performance of the devices was evaluated for analysis of the three analytes. For water hardness, the linear range of 25-1501 mg/L with the limit of detection (LOD) of 13 mg/L visible to the naked eye were obtained with %RSD ranging from 0.54-5.77% and 0.79-4.87% of measuring radial distances in the center and edges of the test area, respectively. The chloride test covers a linear range of 1-100 mM, with a LOD=0.25 mM visible to the naked eye. %RSD for chloride detection ranges from 0.82-6.33% and 1.32-8.03% of measuring radial distances in the center and edges of the test area, respectively. For iron testing, the linear range of 0.5-300 mg/L, with a LOD=0.5 mg/L visible to the naked eye. %RSD for iron detection ranges from 0.27-2.13% and 0.31-7.57% of measuring radial distances in the center and edges of the test area, respectively. Water samples were analyzed for water hardness content and chloride in all 10 water samples, comparing results with traditional methods. The results obtained from the two methods were similar indicating the accuracy the developed paper-based assay. For iron analysis in water samples, a recovery range of 90−104% for all samples was obtained, indicating acceptable accuracy in Fe^{2+} analysis using the developed device. The stability of the prepared devices was evaluated under various storage conditions and storing the device in the fridge maintains a radial distance similar to that of freshly prepared devices for over two months.

These results indicate that the developed paper-based test could serve as a fast and affordable method for on-site determination of water hardness, chloride and iron in water in the future. The paper-based sensor presented demonstrates high sensitivity, low cost, and simultaneous detection of water hardness, chloride, and iron in real water samples.

5.2 Future perspective

Various water samples collected from various sources and locations will be evaluated to study the wide range of applications. Longer shelf-life stability will be evaluated to ensure that the devices can be store for long time uses. Process of fabrication and reagent deposition will be evaluated to provide mass production.

REFERENCES

© The Open University, O. E. f. t.-p. m. a. o. s., this content is made available under a Creative Commons Attribution-Share Alike 4.0 licence: http://creativecommons.org/licenses/by-sa/4.0/. (2019). DETERMINING THE HARDNESS OF RIVER WATER BY EDTA TITRATION. *penSTEM Africa, 1-20*.

Abkenar, S. D., Dahaghin, Z., Sadeghi, H. B., Hosseini, M., & Salavati-Niasari, M. (2011). Determination of zinc in water samples by flame atomic absorption spectrometry after homogeneous liquid-liquid extraction. *Journal of Analytical Chemistry, 66*(6), 612-617. doi:10.1134/s1061934811060062

Akhtar, M. J., Siddiqui, K. S., Rehman, A., & Iqbal, J. . (2022). Glycine: A versatile and multi-functional amino acid. *Advances in Protein Chemistry and Structural Biology, 135, 1-29*.

Al-Khashman, O. A., Alnawafleh, H. M., Jrai, A. M. A., & Al-Muhtaseb, A. a. H. (2017). Monitoring and Assessing of Spring Water Quality in Southwestern Basin of Jordan. *Open Journal of Modern Hydrology, 07*(04), 331-349. doi:10.4236/ojmh.2017.74019

AL-KHATEEB, R. (2014). NFLUENCE OF CHLORIDE CONCENTRATION ON WATER QUALITY. *International Journal of Applied Engineering Research and Development (IJAERD), 63-68*.

Aryal, P., Brack, E., Alexander, T., & Henry, C. S. (2023). Capillary Flow-Driven Microfluidics Combined with a Paper Device for Fast User-Friendly Detection of Heavy Metals in Water. *Anal Chem, 95*(13), 5820-5827. doi:10.1021/acs.analchem.3c00378

Bigham, T., Dooley, J. S. G., Ternan, N. G., Snelling, W. J., Héctor Castelán, M. C., & Davis, J. (2019). Assessing microbial water quality: Electroanalytical approaches to the detection of coliforms. *TrAC Trends in Analytical Chemistry, 121*. doi:10.1016/j.trac.2019.115670

Cate, D. M., Noblitt, S. D., Volckens, J., & Henry, C. S. (2015). Multiplexed paper analytical device for quantification of metals using distance-based detection. *Lab on a Chip, 15*(13), 2808-2818. doi:10.1039/c5lc00364d

Charleton, K. D., Smith, A. E., & Goltz, D. M. (2009). Microsampling and Determination of Metals in Iron Gall Ink. *Analytical Letters, 42*(16), 2533-2546. doi:10.1080/00032710903243570

Di Leo, G., & Sardanelli, F. (2020). Statistical significance: p value, 0.05 threshold, and applications to radiomics-reasons for a conservative approach. *Eur Radiol Exp, 4*(1), 18. doi:10.1186/s41747-020-0145-y

Dvorak, B. (2021). Drinking Water: Iron and Manganese. *NebGuide, 1-6*.

DWAF. (1996a). SOUTH AFRICAN WATER QUALITY GUIDELINES. *Department of Water Affairs and Forestry, Pretoria, South Africa, Volume 7, Aquatic ecosystems*.

DWAF. (1996b). SOUTH AFRICAN WATER QUALITY GUIDELINES. *Department of Water Affairs and Forestry, Pretoria, South Africa, Volume 1, Domestic use*.

El-Turki, I. E. S. a. K. S. (2017). Iron determination of drinking water wells in Benghazi City. *Quest Journals, 47-53*.

Gaur, N., Sarkar, A., Dutta, D., Gogoi, B. J., Dubey, R., & Dwivedi, S. K. (2022). Evaluation of water quality index and geochemical characteristics of surfacewater from Tawang India. *Sci Rep, 12*(1), 11698. doi:10.1038/s41598-022-14760-3

Gemma Aragay, H. M., Josefina Pons, Mercè Font-Bardíac and Arben Merkoçi. (2012). Rapid and highly sensitive detection of mercury ions using a fluorescence-based paper test strip with an N-alkylaminopyrazole ligand as a receptor. *Journal of Materials Chemistry, 22(13)*.

Gwak, D. S., Chung, I., Kim, B. K., Lee, S., Jeong, H. G., Kim, Y. S., . . . Han, M. K. (2021). High Chloride Burden and Clinical Outcomes in Critically Ill Patients With Large Hemispheric Infarction. *Front Neurol, 12*, 604686. doi:10.3389/fneur.2021.604686

Hames, B. D. (2017). Gel Electrophoresis of Proteins. *A Practical Approach*.

Harvey Jr, A. E., Smart, J. A., & Amis, E. S. . (1955). Simultaneous Spectrophotometric Determination of Iron(II) and Total Iron with 1,10-Phenanthroline. *Analytical Chemistry, 27(1), 26-29*.

Hiroki Tamura, K. G., Takao Yotsuyanagi, and Masaichi Nagayama. (1974). Spectrophotometric determination of iron(II) with 1,10-phenanthroline in the presence of large amounts of iron(III). *Talanta, 21(4), 314–318*.

Husain, A. (2017). COMPLEXOMETRIC TITRATIONS. *Pharmaceutical Analysis, 1-34*.

Izzo, M., Masetti, M., & Focarete, M.L. (2016). Development of biocompatible gelatin/CAPS hydrogels as scaffolds for tissue engineering. *Journal of Applied Polymer Science, 133(2), 42699.*

J. Bartram, R. B. a. D. C. (1999). Major Ions in Water. *Hydrology Project Training Module File, 1-41*.

Jayaraman, P., Nagarajan, K. K., Partheeban, P., & Krishnamurthy, V. (2024). Critical review on water quality analysis using IoT and machine learning models. *International Journal of Information Management Data Insights, 4*(1). doi:10.1016/j.jjimei.2023.100210

Karita, S., & Kaneta, T. (2016). Chelate titrations of Ca(2+) and Mg(2+) using microfluidic paper-based analytical devices. *Anal Chim Acta, 924*, 60-67. doi:10.1016/j.aca.2016.04.019

Kaur, P., Sharma, G., & Singh, R. (2020). Development and validation of a rapid titration method for the determination of bromide ions in pharmaceutical formulations. *Analytical Methods, 12(5), 752-759.*

Koronkiewicz, S. (2021). Photometric Determination of Iron in Pharmaceutical Formulations Using Double-Beam Direct Injection Flow Detector. *Molecules, 26*(15). doi:10.3390/molecules26154498

Korte, D., Tomsič, G., Bratkič, A., Franko, M., & Budasheva, H. (2019). Determination of Iron in Environmental Water Samples by FIA-TLS. *Acta Chimica Slovenica,* 814-820. doi:10.17344/acsi.2018.4825

Liu, K. K., Wu, R. G., Chuang, Y. J., Khoo, H. S., Huang, S. H., & Tseng, F. G. (2010). Microfluidic systems for biosensing. *Sensors (Basel), 10*(7), 6623-6661. doi:10.3390/s100706623

Maria Smolinska, O. K., Teodozia Vrublevska and Grigory Teslyar. (2015). ERIOCHROME BLACK T – A NEW ANALYTICAL REAGENT FOR

SPECTROPHOTOMETRIC DETERMINATION OF SULPHANILAMIDES. *CHEMISTRY & CHEMICAL TECHNOLOGY, Vol. 9, No. 4*.

Maurya, R. (2023). The Potential of Environmental Benefits of Urban Agriculture and Their Future. *ResearchGate, 127-130*.

Menger, R. F., Beck, J. J., Borch, T., & Henry, C. S. (2022). Colorimetric Paper-Based Analytical Device for Perfluorooctanesulfonate Detection. *ACS ES&T Water, 2*(4), 565-572. doi:10.1021/acsestwater.1c00356

Nilghaz, A., Wicaksono, D. H., Gustiono, D., Abdul Majid, F. A., Supriyanto, E., & Abdul Kadir, M. R. (2012). Flexible microfluidic cloth-based analytical devices using a low-cost wax patterning technique. *Lab Chip, 12*(1), 209-218. doi:10.1039/c1lc20764d

Nouanthavong, S., Nacapricha, D., Henry, C. S., & Sameenoi, Y. (2016). Pesticide analysis using nanoceria-coated paper-based devices as a detection platform. *Analyst, 141*(5), 1837-1846. doi:10.1039/c5an02403j

Olowu, R. A., Ayejuyo, O. O., Adewuyi, G. O., Adejoro, I. A., Akinbola, T. A., Osundiya, M. O., & Onwordi, C. T. (2010). Assessment of Pollution Trend of Oke Afa Canal Lagos, Nigeria. *E-Journal of Chemistry, 7*(2), 605-611. doi:10.1155/2010/949017

Oyewunmi, O. D., Safiabadi-Tali, S. H., & Jahanshahi-Anbuhi, S. (2020). Dual-Modal Assay Kit for the Qualitative and Quantitative Determination of the Total Water Hardness Using a Permanent Marker Fabricated Microfluidic Paper-Based Analytical Device. *Chemosensors, 8*(4). doi:10.3390/chemosensors8040097

Pholprasert, P. (2002). Water Quality Management in Thailand. *Journal of Environmental Management, 64(3), 237-247*. doi:10.1006/jema.2001.0505

R. Rajendran1, A. P. R., A. Sahaya Raja1, V. Prathipa2 , M.S. Dheenadayalan1,*. (2015). Assessment of Physico–Chemical Parameters of River Cauvery In and Around Nerur. *Journal of Environmental Science and Pollution Research, 17–19*.

Rahbar, M., Paull, B., & Macka, M. (2019). Instrument-free argentometric determination of chloride via trapezoidal distance-based microfluidic paper devices. *Anal Chim Acta, 1063*, 1-8. doi:10.1016/j.aca.2019.02.048

Sarma, S. T. a. K. (2018). Assessment of Groundwater Quality in Different Land Uses in Ghaziabad District of Uttar Pradesh, India. *Available online at www.ewijst.org, 99-117*.

Sengupta, P. (2013). Potential Health Impacts of Hard Water. *International Journal of Preventive Medicine (IJPM), 866-875*.

Sharifi, H., Tashkhourian, J., & Hemmateenejad, B. (2020). A 3D origami paper-based analytical device combined with PVC membrane for colorimetric assay of heavy metal ions: Application to determination of Cu(II) in water samples. *Anal Chim Acta, 1126*, 114-123. doi:10.1016/j.aca.2020.06.006

Shibata, H., Hiruta, Y., & Citterio, D. (2019). Fully inkjet-printed distance-based paper microfluidic devices for colorimetric calcium determination using ion-selective optodes. *Analyst, 144*(4), 1178-1186. doi:10.1039/c8an02146e

Sriram, G., Bhat, M. P., Patil, P., Uthappa, U. T., Jung, H.-Y., Altalhi, T., . . . Kurkuri, M. D. (2017). Paper-based microfluidic analytical devices for colorimetric detection of toxic ions: A review. *TrAC Trends in Analytical Chemistry, 93*, 212-227. doi:10.1016/j.trac.2017.06.005

Taprab, N., & Sameenoi, Y. (2019). Rapid screening of formaldehyde in food using paper-based titration. *Anal Chim Acta, 1069*, 66-72. doi:10.1016/j.aca.2019.03.063

Tasaengtong, B., & Sameenoi, Y. (2020). A one-step polymer screen-printing method for fabrication of microfluidic cloth-based analytical devices. *Microchemical Journal, 158*. doi:10.1016/j.microc.2020.105078

Tasangtong, B., Pholsaptanakorn, T., Tapsawut, T., Wiwekwin, N., Mettakoonpitak, J., Na Nongkhai, P., & Sameenoi, Y. (2024). User-friendly diameter-based measurement paper sensor for chloride detection in water. *Talanta Open, 9*. doi:10.1016/j.talo.2024.100305

Thatai, S., Verma, R., Khurana, P., Goel, P., & Kumar, D. (2019). Water Quality Standards, Its Pollution and Treatment Methods. In *A New Generation Material Graphene: Applications in Water Technology* (pp. 21-42).

University of Canterbury, T. W. W. o. W. C. N. Z. Determination of Chloride Ion Concentration by Titration (Mohr's Method). *College of Science, 1-2*.

Véronique Rouchon a, Maroussia Duranton a, Oulfa Belhadj a, Marthe Bastier-Deroches a, Valéria Duplat a,b, Charlotte Walbert a, Birgit Vinther Hansen b. (2013). The use of halide charged interleaves for treatment of iron gall ink damaged papers. *Polymer Degradation and Stability, 98, 1339-1347.*

Vinutha, N. K., Ravishankar, B., & Avadhani, G. S. (2018). Adsorption Indicator Titration of Halides: An Experiment for Teaching Precipitation Titrations. *Journal of Chemical Education, 95(6), 1076-1079*.

Wang, J., Li, H., Li, X., & Zhang, L. (2021). Rapid determination of chloride ions in seawater by Mohr's titration. *ANALYTICAL SCIENCES, 37(7), 929-933.*

Wu, D., Hu, Y., Liu, Y., & Zhang, R. (2021). Review of Chloride Ion Detection Technology in Water. *Applied Sciences, 11*(23). doi:10.3390/app112311137

Yetisen, A. K., Akram, M. S., & Lowe, C. R. (2013). Paper-based microfluidic point-of-care diagnostic devices. *Lab Chip, 13*(12), 2210-2251. doi:10.1039/c3lc50169h

ต้นฉบับไม่ปรากฏหน้านี้